

Editorial Board

Dr. Mohammad I. Malkawi

Associate Professor, Department of Software Engineering

Jordan

Dr. Kaveh Ostad-Ali-Askari

Assistant Professor, Department of Civil Engineering, Isfahan (Khorasgan) Branch,

Iran

Dr. Mohammed A. Akour

Associate Professor in the Department of Software Engineering,

Jordan

Dr. Mohammad mehdi hassani

Faculty of Computer Engineering

Iran

Prof. Ratnakaram Venkata Nadh (Ph.D)

Professor & Head - Chemistry Department, Dy. Director - Admissions

India

Dr. SIDDIKOV ILKHOMJON KHAKIMOVICH

Head of the Department of "Power Supply Systems",

Uzbekistan

Dr. S. DHANASEKARAN

Associate Professor in the Department of Computer Science and Engineering,

India

Younes El Kacimi, Ph. D.

Science Faculty, Department of Chemistry Kénitra

Morocco

Denis Chemezov

Lecturer, Vladimir Industrial College, Vladimir

Russia

RICHARD O. AFOLABI, Ph.D.

Department of Petroleum Engineering,

Nigeria

Volume 3 ISSUE 3

July-August 2019

Automated Detection of Manhole Status and Prevention of Accidents Using PIR Sensors

S.PRIYADHARSINI || T.VARSHA

Sucrose Crystallization: Modeling of Thermodynamic Equilibrium in Impure Aqueous Solutions

Abdelali BORJI || Fatima-Ezzahra BORJI || Abdelaziz JOURANI

Isolation and characterization of polycyclic aromatic hydrocarbon degrading bacteria From contaminated soil sludge in Tamilnadu

T. Velayutham

Phosphate Industry: Gypsum Crystallization under the Industrial Conditions of Wet-Process Phosphoric Acid Production

Fatima-Ezzahra BORJI || Abdelali BORJI || Abdelaziz JOURANI

Design of Mobile Meteorological Station with Embedded System Control

Ahmet Kayabasi || Berat Yildiz || Kadir Sabanci || Abdurrahim Toktaş || Mehmet Yerlikaya

Automated Detection of Manhole Status and Prevention of Accidents Using PIR Sensors

S.PRIYADHARSINI, T.VARSHA

Department of Computer Science and Engineering

Velammal Engineering College, Chennai

ABSTRACT

Manholes are essential aspects of a city's infrastructure. Damaged manholes are posing a threat to commuters in city. Some of the damaged manholes can be seen on the busiest roads of the city. Many of them are not properly closed and can cause serious accidents. Fatal accidents caused due to open potholes are upsurging day by day. Passers by are at a high risk of facing hazards while crossing these manholes that are either damaged or kept open by the sanitation workers. This paper proposes a novel technique of affixing a passive infrared sensor at the pro-ring of the manhole chamber. WiiLSW are used to detect if the man-hole is open or closed. The PIR sensor is activated only if the man-hole is open. The sensor is attached to a security alarm circuit which is activated when a human intrigues the sensing area of the sensor, thus serves as a warning to those who seem to carelessly walk over the potholes and might save them from falling into the manhole. This alarm circuit also produces vibrations making it easy for deaf persons too. This whole set up can be implemented effectively using inexpensive equipment.

I. Introduction

In a recent survey conducted by National Crime Records Bureau 780 people have died on account of accidental fall into open manholes. Uncovered, unprotected open manholes have killed as many as 167 persons and injured five in 2018.



Besides being a threat to pedestrians, the uncovered manholes and pothole-riddled roads are posing serious threats to motorists. According to the Environmental Protection Agency, there are approximately 12 million sewer or storm water manholes across the nation. The surprising fact is that out of these nearly 12 million manholes, the Public Works Magazine estimates 80% need some level of maintenance or rehabilitation.

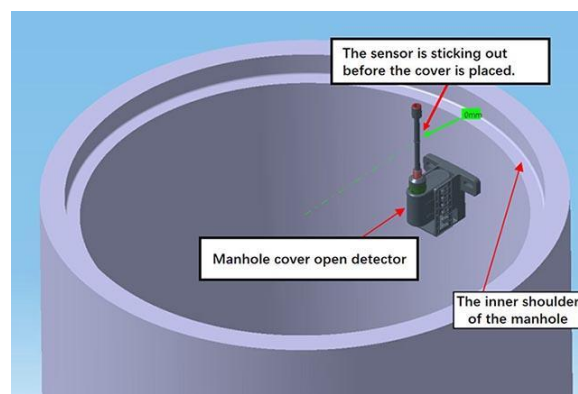
Measures are not being taken for closing such manholes and other death traps or barricading them. This is simply due to the lack of accountability, absence of safety consciousness and sheer

insensitivity to human tragedy. One of the major reasons for open potholes is the theft of the manhole covers leaving the manhole chambers open and unattended. Despite placing warning flags on the manhole covers, In floodwaters a person may not see the open drains and so risks falling in.

Falling into an open sewer can cause a myriad of dangers which may be as serious as suffocation to death. Toxic gases resulting from cleaning fluids and excrement may cause severe risks to those breathing them. The septic environment poses severe risk of infection to the victim if he or she happened to have any open cuts. Oxygen levels are very low especially in deeper sewers.

Sewer gas present inside is a complex combination of various organic and inorganic compounds which is the result of the breakdown of human waste in the absence of oxygen. Excessive inhalation of this gas may cause delirium, or even unconsciousness. For this reason it is considered to be an asphyxiant, and dangerous in enclosed spaces.

II. WiiLSW sensors

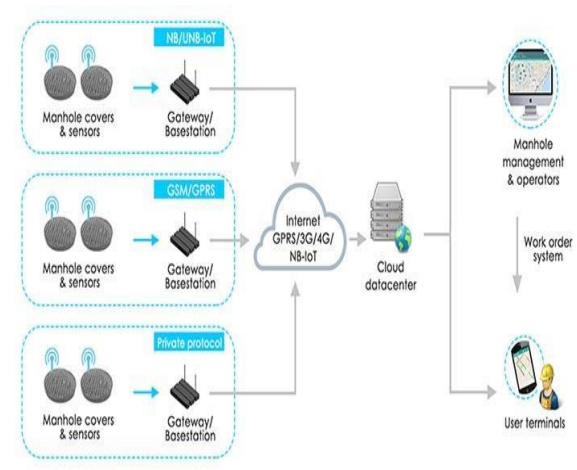


WiiLSW ,a positioning sensor in the WiiHey family designed to be extremely tamper resistant sealed and rugged for use in even unconventional environments. With the utilization of the off-shelf sensors, it is trying to be a zero-false alarm solution

Working

The sensor detects two statuses of the manhole cover-open or closed. During installation, the sensor is sticking out of the manhole surface, indicating the manhole is in "opened" status. After the manhole cover is placed on it, the sensor is bending over, knowing now the manhole is in "closed" status.

Architecture



The sensor supports LPWAN IoT communications technologies, such as GPRS, NB-IoT, GPRS, etc. They combine high transmission ranges of up to several kilometers in urban environments, with low power consumption. Data are transmitted to cloud data center for processing and fusion. Eventually, operators could view every manhole status from a cloud-based GIS dashboard.

III. PROPOSED IDEA

WiiHey's Manhole cover Open Detector is used initially, the realtime manhole status data is transmitted from the sensor to the cloud database via(LPWAN)Low Power Wide Area Network.This integration provides a web based GIS dashboard platform to monitor and plan the maintenance of the assets.

IV. Passive Infrared Sensor

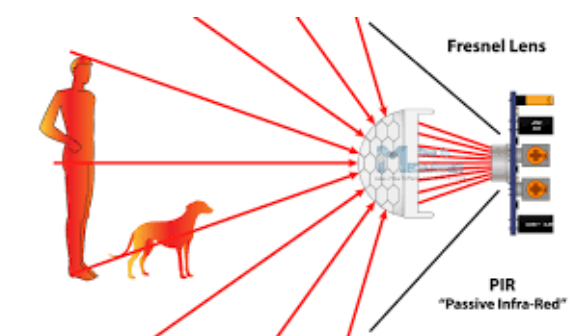
The ultimate purpose of PIR sensor is to sense motion. This sensor is used to detect whether a human has moved in or out of the sensors range.

This sensor detects a human being moving around within approximately 10m from the sensor.

It is used to discover the entry and exit of an individual within the specified sensor area. These are small, cheap, easy to use, consume low power and do not wear out very easily.

These pyroelectric sensors are can detect levels of infrared radiation. It measures the temperature, the hotter something is, the more radiation is emitted. It passively detects the infrared radiation coming from the human body in the surrounding area. The detected radiations are then converted into an electrical charge, which is proportional to the detected level of the radiation.

Working of PIR Sensors



PIR sensor consists of a specially designed cover named Fresnel lens, which focuses the infrared signals onto the pyroelectric sensor. It consists of two slots which are made up of a special material sensitive to IR. Both slots detect the same amount of IR.

When the sensor detects the motion of a warm body like human or an animal one half of the PIR sensor is interrupted at first, which causes a positive differential change between the two halves. Similarly when the body leaves the sensing area, the reverse process takes place. In this case a negative differential change is created.

As the motion is detected, the output pin will go high to 3.3V. This electrical signal can be used to activate an alert system or buzzer or alarm sound.

The PIR sensor can be fixed at the pro-ring of the manhole chamber. So that it can detect the motion of humans moving nearby or very close to the manhole. If the motion of a human or an animal is detected very close to the manhole chamber, such that the motion intrigues the sensing area of the sensor, then the sensor is activated electrical pulses are generated which is fed into the inverter circuit and the alarm system is activated.

This alarm serves as a warning to those who seem to carelessly walk over the potholes and might save them from falling into the manhole. Even if a human or an animal has fallen into the pothole accidentally, the sensor detects the presence of the person due to infrared radiation emitted by the hot body and the alarm system is activated . In this way, unfortunate accidents due to fall into potholes can be prevented.

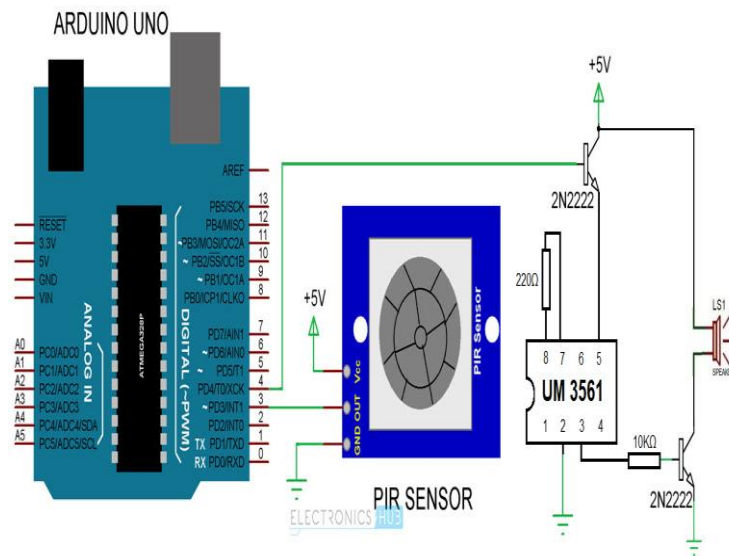
This whole set up can be implemented using inexpensive equipment which consume low power. These equipments do not wear out and are easy to handle making the process easier for maintenance.

V. PIR Sensor based Security Alarm Circuit Design

The PIR sensor is connected to the alarm system. The designed system consists of Arduino, PIR sensor, UM3561 IC, Speaker, transistor and a couple of resistors. The UM3561 IC is a Siren generator IC. It has 8 pins. First and sixth pins are the Sound effect selection Pins.

Pin 5 is connected to +5V through an NPN Transistor. 220K Ω resistor is connected to the seventh pin of the UM 3561 IC and the other end is connected to the eighth pin of the IC. Output is taken from the third pin of the IC and it is connected to a speaker through a resistor and transistor. The base of the transistor is connected to the output of the IC through a resistor of 10K Ω . Emitter pin is connected to the ground while one end of the speaker is connected to the collector, while the other end is connected to +5V. Output of the PIR sensor is connected to the Pin 3 of Arduino.

Working of PIR sensor based security alarm



1. The connections are made as per the circuit diagram.
2. The PIR sensor is powered and it detects the IR rays emitted from humans within the sensing area.
3. This PIR sensor has a range of 5 meters. This distance can be varied.
4. When the presence of a human is detected, the PIR sensor outputs a logic HIGH value i.e. voltage of 3.5V to 5V to Arduino's Pin 3.
5. As soon as the Arduino detects logic HIGH on Pin 3, it makes the Pin 4 HIGH for a duration of 10S. During this time, the Siren IC UM3561 is activated as its Pin 5 provided with +5V.
6. This siren generator has an oscillator internally, to produce the sound and the oscillator is tuned to a certain frequency and using a 220KΩ resistor.
7. The oscillations are sent to the address counter. The address counter then sends the data to the ROM.
8. ROM then sends the alarm tone on the output pin 3.
9. The output is given to the NPN transistor to amplify the siren.
10. The base of the transistor gets voltage from output pin of the siren generator.
11. Transistor starts conducting when it gets the cutoff voltage at the base and the speaker is negative pin and is connected to the ground.
12. Thus sound produced can be heard from the speaker when human is likely to cross the manhole at a much closer distance.
13. It also produces a great vibration making it easy to give away a warning for deaf persons too.

VI. Conclusion

The combination of the WiiLSW sensor along with PIR sensor for preventing accidents due to careless handling of manhole can be greatly reduced.

WiiHey's Manhole cover Open Detector permitting low power consumption optimises the usage over any remote location. The PIR uses the infrared radiations which is a electromagnetic radiation that can be easily created using commercially available devices. It produces vibration which will alert even a deaf person when they accidentally come near the vicinity of an opened manhole.

VII. References

- [1] <https://ieeexplore.ieee.org/document/1033761>
- [2] <http://www.wiihey.com/en/applications/manhole-cover-monitoring.html>
- [3] <http://www.embeddedworks.net/sens377.html>
- [4] <https://www.elprocus.com/pir-sensor-circuit-with-working/>
- [5] <https://howtomechatronics.com/tutorials/arduino/how-pir-sensor-works-and-how-to-use-it-with-arduino/>
- [6] <http://www.glolab.com/pirparts/infrared.html>
- [7] <https://www.nap.edu/read/4782/chapter/7#35>
- [8] <https://howtomechatronics.com/tutorials/arduino/how-pir-sensor-works-and-how-to-use-it-with-arduino/>

Sucrose Crystallization: Modeling of Thermodynamic Equilibrium in Impure Aqueous Solutions

Abdelali BORJI^{1,*}, Fatima-Ezzahra BORJI¹ and Abdelaziz JOURANI¹

¹Laboratory of Physical Chemistry of Processes and Materials, Department of Applied Chemistry and Environment
Faculty of Sciences and Techniques, University Hassan 1
Settat, Morocco

ABSTRACT

Crystallization is an important process in industrial operations. In sugar manufacturing, crystallization is a crucial step that determines the quality of the final product, which requires control of its fundamental parameters especially thermodynamic parameters. In fact, to study the crystallization of sucrose, it is extremely important to know the sucrose solubility, which reflects a thermodynamic equilibrium, and how it can vary in the presence of non-sucrose (impurities). Indeed, in crystallization, solubility is of fundamental importance in the definition of supersaturation which is the driving force of crystallization. In this study, the sucrose solubility has been modeled as a function of sucrose concentration, mass percentage of glucose and fructose applying a full factorial design. The validation of the developed model was verified by additional batch experiments. The results confirm that the proposal model provided a satisfactory fit to the experimental data. The results also show the decrease in the sucrose solubility with the increase in the mass percentage of glucose and fructose.

Keywords—*thermodynamic equilibrium; crystallization; sucrose; fructose; glucose; experimental design.*

I. INTRODUCTION

Crystallization is a separation and purification process frequently employed in the industry, particularly in the sugar industry [1]. Two crucial parameters in crystallization are temperature and solvent. The solvent affects the solubility of the crystals, which constitutes the basis for any crystallization process [2-5]. The solubility concentration and its dependence on temperature determine the yield of the process and the generation of supersaturation (driving force of crystallization) [6, 7]. Solubility reflects a thermodynamic equilibrium in which the chemical potential of the solute is equal to the chemical potential of the solid phase [8]. To be able to control a crystallization process we need to know the solubility of the different solid forms and how they are related to the solvent and temperature [9]. In the sugar industries the impurities or non-sucrose found in the sugar juice affect the sucrose solubility which influences the sucrose crystallization and consequently the quality of the sucrose produced will be impacted [10-12]. So to deal with the problems related to crystallization process, it is extremely important to master the sucrose solubility in the presence of impurities. For this, in this study, the sucrose solubility will be modeled as a function of sucrose concentration and in presence of glucose and fructose as impurities using the experimental design method especially the full factorial design.

II. EXPERIMENTAL SECTION

Sucrose, glucose and fructose employed are "of analytical" quality to avoid any other impurities which may influence the measurements. Distilled water is used as solvent. The experiments were conducted in a jacketed reactor with a mechanical stirrer. A cryothermostat has been used for temperature control. The temperature in the reactor is controlled by a digital thermometer. The cooling is carried out by a cryothermostat and the determination of the solubility is performed using the spectrophotometric method [10].

III. RESULTS AND DISCUSSIONS

A method to illustrate the influence of impurities on the sucrose solubility is to follow the deviation from the thermodynamic equilibrium, in other words the difference between the solubility in a pure system and that in the case of the presence of impurities. In this study and in order to elucidate the effect of glucose and fructose additives on the sucrose solubility in water, this deviation has been modeled as a function of sucrose concentration, mass percentage of glucose and mass percentage of fructose using the experimental design method especially the full factorial design [13]. The experimental design is a powerful method of experimentation which presents a complex system in the form of mathematical equations. The experimental design helps to study the effects caused by independent factors and their interactions [14]. If we call n the number of variables to be tested, in order to measure the effect of all the variables combinations when each variable is tested at a high and a low level, 2^n experiments will be needed [15]. Two levels for each factor have been selected according to the average composition of the sugarcane [16]. The natural values of each factor and their respective levels are presented in Table I. The different experiments performed in this study are shown in Fig.1.

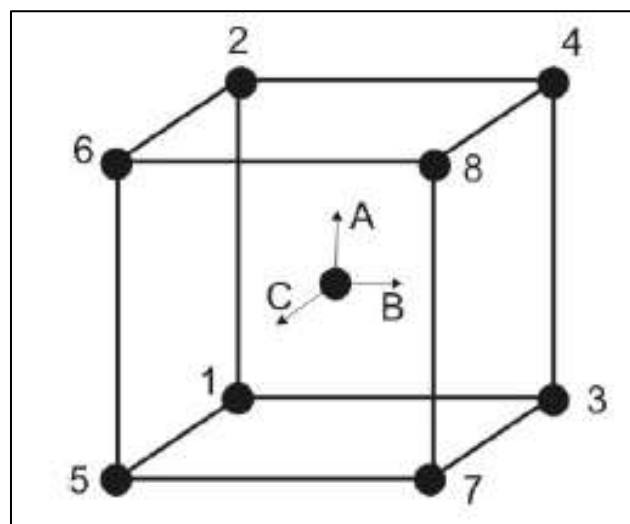


Fig.1. 2^3 full factorial design.

TABLE I. THE EXPERIMENTAL RANGES AND LEVELS OF INDEPENDENT VARIABLES.

Factors	Symbol	Low level (-1)	High level (+1)	Unit
Concentration of sucrose	X_1	220	240	g/100g water
Mass percentage of glucose	X_2	0.05	0.15	% weight
Mass percentage of fructose	X_3	0.05	0.15	% weight

The behavior of the system is explained by the following model:

$$\hat{y} = a_0 + \sum_{i=1}^k a_i x_i + \sum_{i=1}^k \sum_{j=1}^k a_{ij} x_i x_j + \varepsilon \quad (1)$$

Where \hat{y} is the response (dependent variable), a_0 is the value of fitted response at the center point of design, a_i is the linear effect and a_{ij} is the interaction terms. It should be noted that the x_i is the coded value of the i^{th} variable. The coded values were obtained from the following relationship [17-19]:

$$x_i = \frac{X_i - X_0}{\Delta X_i} \quad (2)$$

With: $X_0 = (X_{i\max} + X_{i\min})/2$; $\Delta X_i = (X_{i\max} - X_{i\min})/2$

Where x_i is the coded value of i^{th} variable, X_i is the encoded value of i^{th} variable, X_0 is the value of X_i at the center point of the investigation domain and ΔX_i is the step size. Here, $X_{i\max}$ and $X_{i\min}$ represent the maximum and the minimum level of factor i in natural unit, respectively. According to full experimental design, 2^3 experiments were conducted and the values of the deviation from the equilibrium (response y) were tabulated (see Table II).

Using Minitab software, the experimental data are analyzed and the following polynomial equation in coded form was established to explain the effect of sucrose concentration, mass percentage of glucose and mass percentage of fructose on the thermodynamic equilibrium in the sucrose crystallization in aqueous solutions.

$$\hat{y} = 15.62 + 1.358x_1 + 3.169x_2 + 7.979x_3 + 0.4769x_1x_2 + 0.6886x_1x_3 + 0.9771x_2x_3 \quad (3)$$

In order to verify the validity of the developed model, several additional batch experiments were carried out in the experimental area of each factor, and each experimental response was compared with the predicted one (see Table III). As Table III shows, the proposed model provided a satisfactory fit to the additional experimental data.

TABLE II. EXPERIMENTAL DESIGN MATRIX.

Experiment	X ₁	X ₂	X ₃	y (g)
1	220	0.05	0.05	5.535
2	240	0.05	0.05	5.373
3	240	0.15	0.05	11.257
4	220	0.05	0.15	17.615
5	240	0.15	0.15	30
6	220	0.15	0.05	8.417
7	220	0.15	0.15	25.5
8	240	0.05	0.15	21.302

TABLE III. MODEL VALIDATION.

Additional Experiment	Observed, y (g)	Estimated, \hat{y} (g)	Error
(0,0,0)	15.525	15.620	0.005
(0.5,0.5,0.5)	22.412	22.408	0.003
(-0.5,-0.5,-0.5)	9.91	9.902	0.007

From equation 3 and according to Vavrincz's equation [20] giving the solubility-temperature dependence, the following model can be deduced to predict the solubility temperature ($T_s, ^\circ C$) as a function of sucrose concentration and mass percentages of glucose and fructose.

$$T_s = 43.59 + 5.788 x_1 + 1.212 x_2 + 3.538 x_3 + 0.1625 x_1 x_2 + 0.08750 x_1 x_3 + 0.6625 x_2 x_3 \quad (4)$$

The values obtained by the model (\hat{y} predicted) are compared with those of experimental data (y experimental) (Table IV). The goodness of fit of the model was checked by the determination coefficient (R^2). In this case, the value of determination coefficient ($R^2 = 0.999$) indicated that only 0.1% of the total variations were not explained by the regression model (see Fig. 2). To verify the systematic departures from the assumptions that errors are normally distributed and are independent of each other and that the error variances are homogeneous, a diagram of residual values by order was constructed (see Fig. 3). The random distribution of residuals confirms their normality and independence.

TABLE IV. COMPARISON BETWEEN OBSERVED AND PREDICTED RESPONSES.

Runs	y	\hat{y}	Residuals
1	21.302	21.0226	0.2794
2	5.535	5.2566	0.2784
3	8.417	8.6866	-0.2696
4	25.5	25.2216	0.2784
5	17.615	17.8832	-0.2682
6	11.257	10.9792	0.2778
7	5.373	5.6416	-0.2686
8	30	30.2686	-0.2686

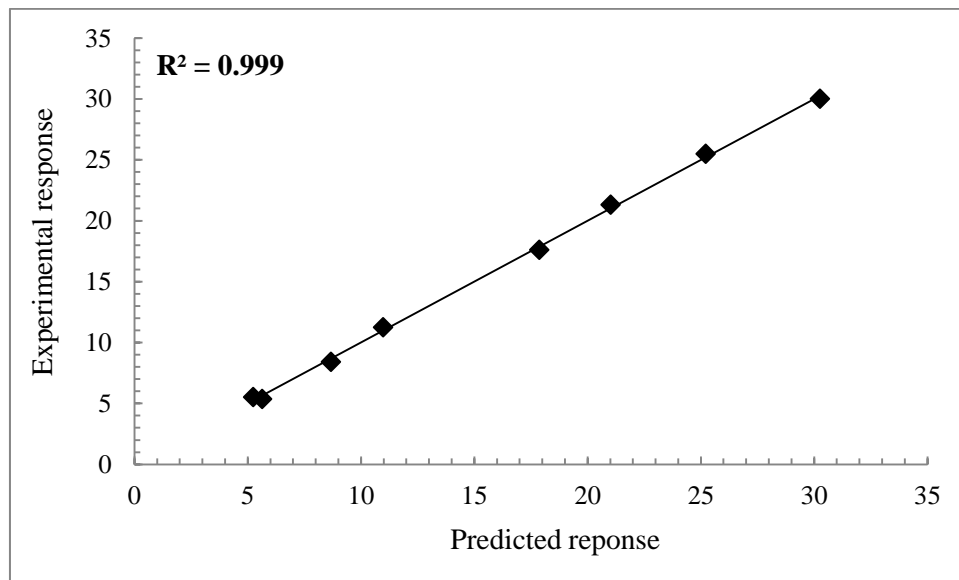


Fig. 2: Comparison of experimental and predicted responses.

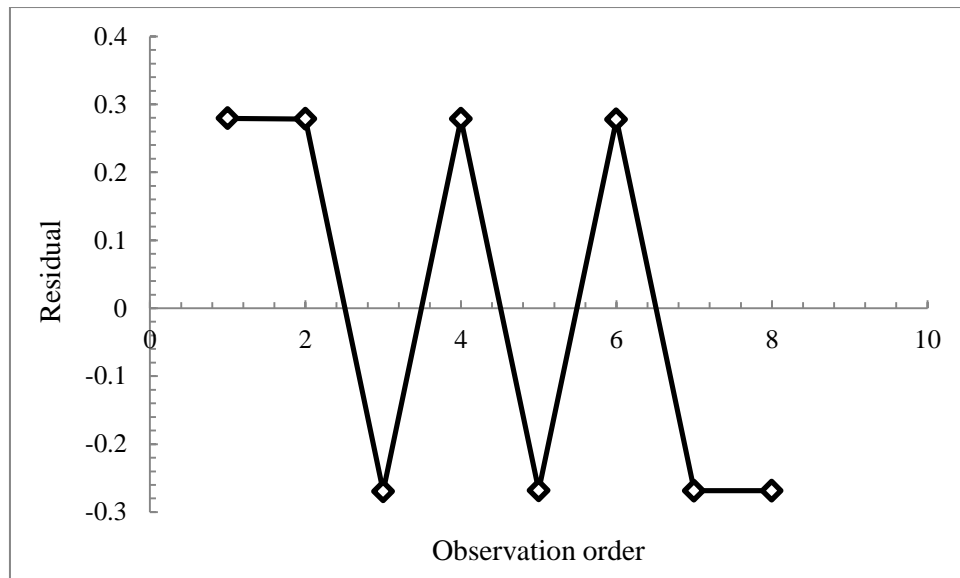
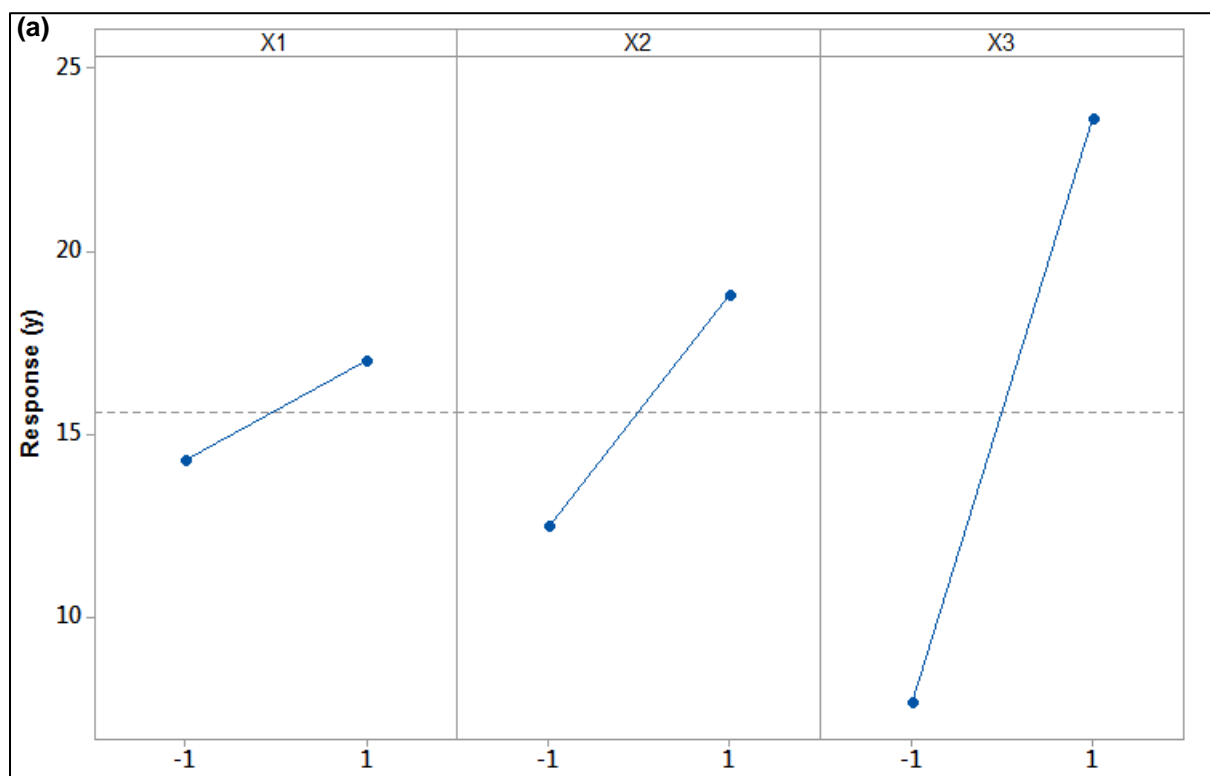


Fig. 3. Residual values according to the order.

To illustrate the effect of sucrose concentration (x_1), mass percentage of glucose (x_2) and mass percentage of fructose (x_3) on the sucrose solubility, the effects diagram and contour plots have been constructed (see Fig. 4 and 5). The results show that the sucrose solubility decreases in the presence of glucose and fructose. This is in good agreement with the results previously published by the authors [10].



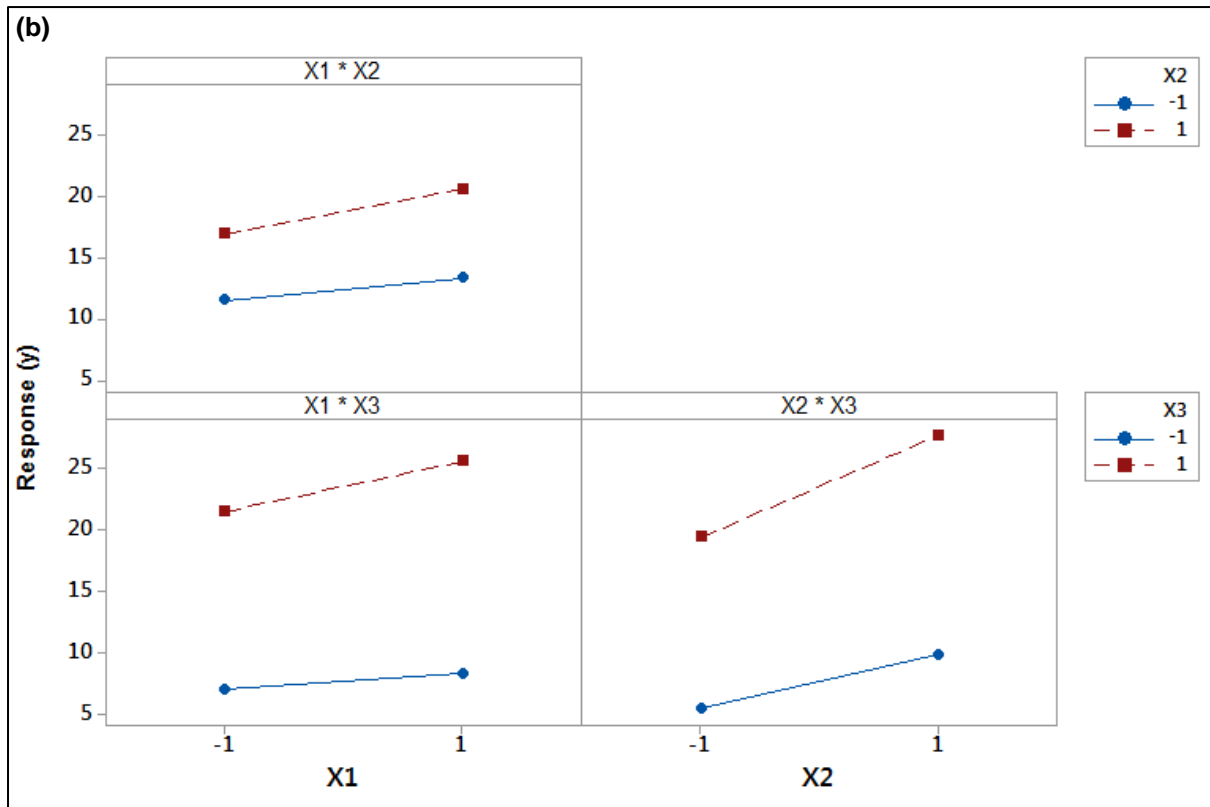
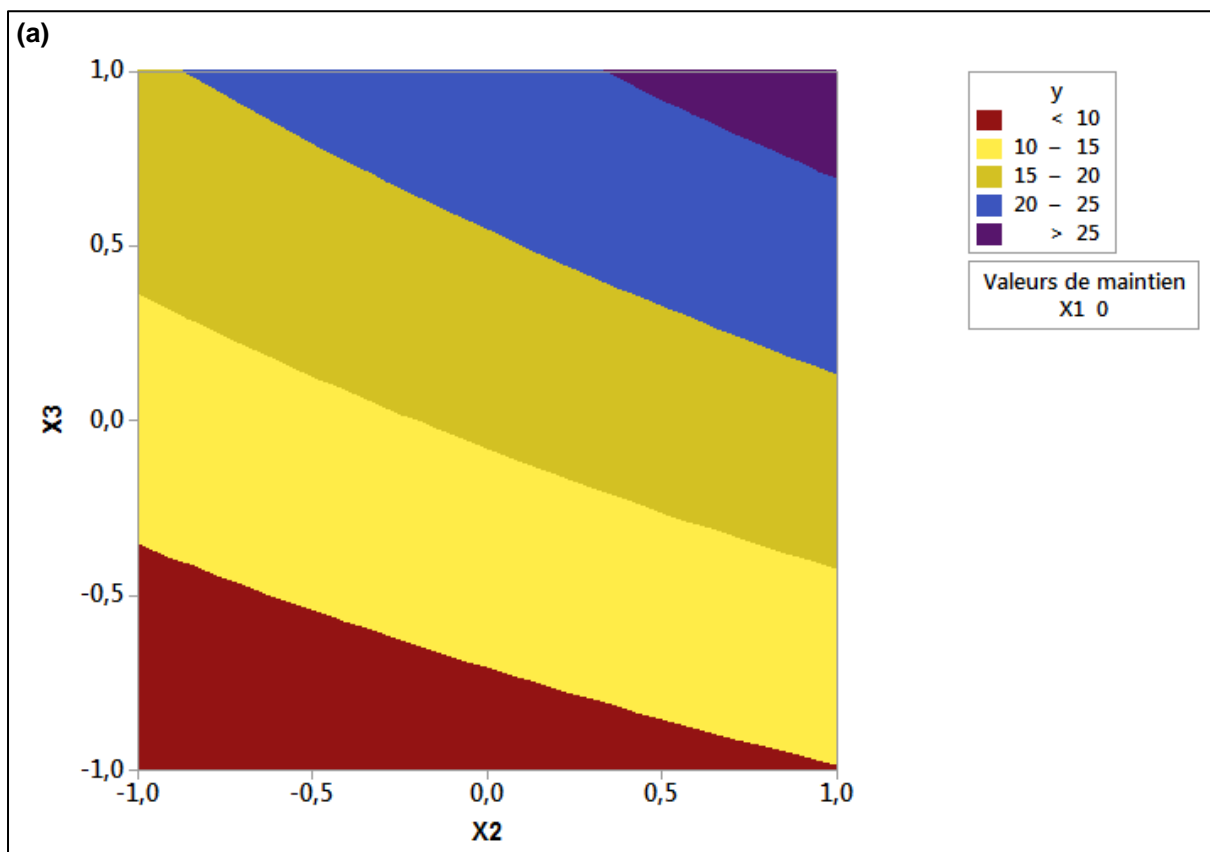


Fig. 4. Effects diagram, (a): main effects of the independent variables, (b) effects of interactions between independent variables.



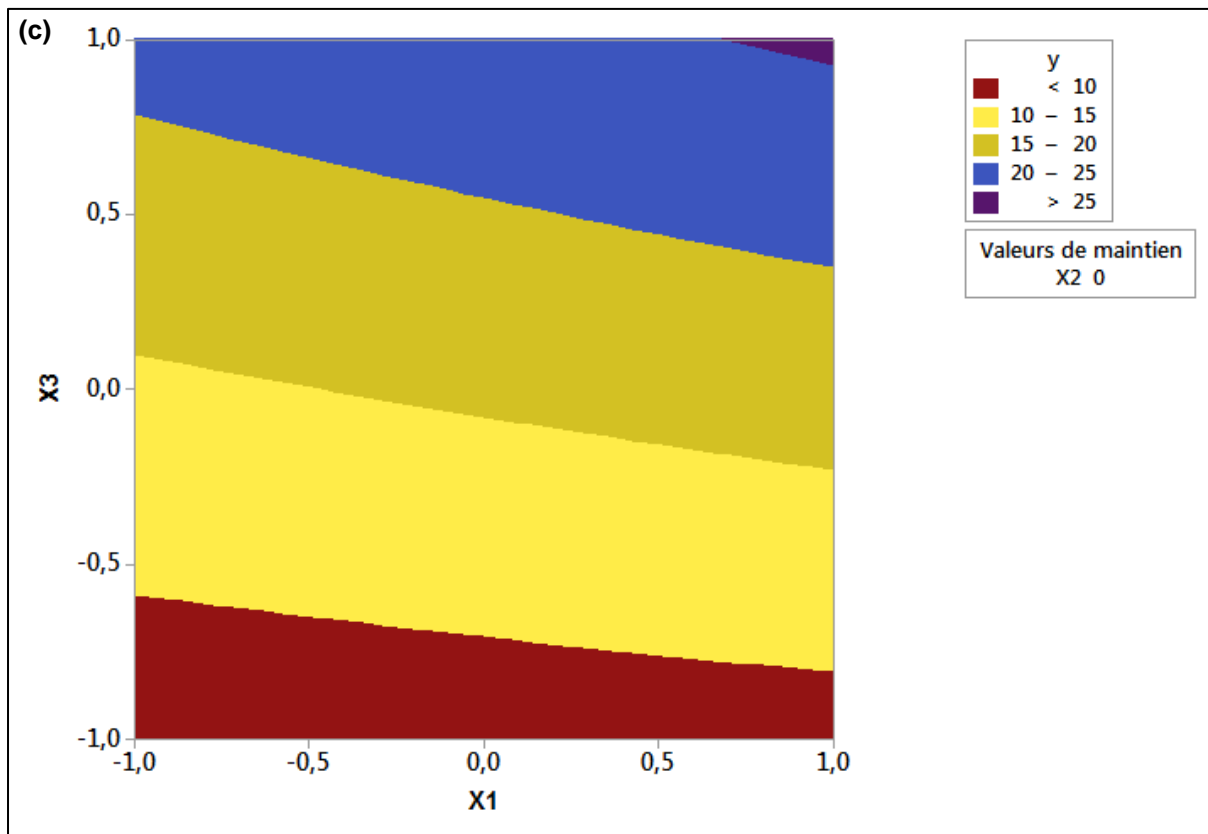
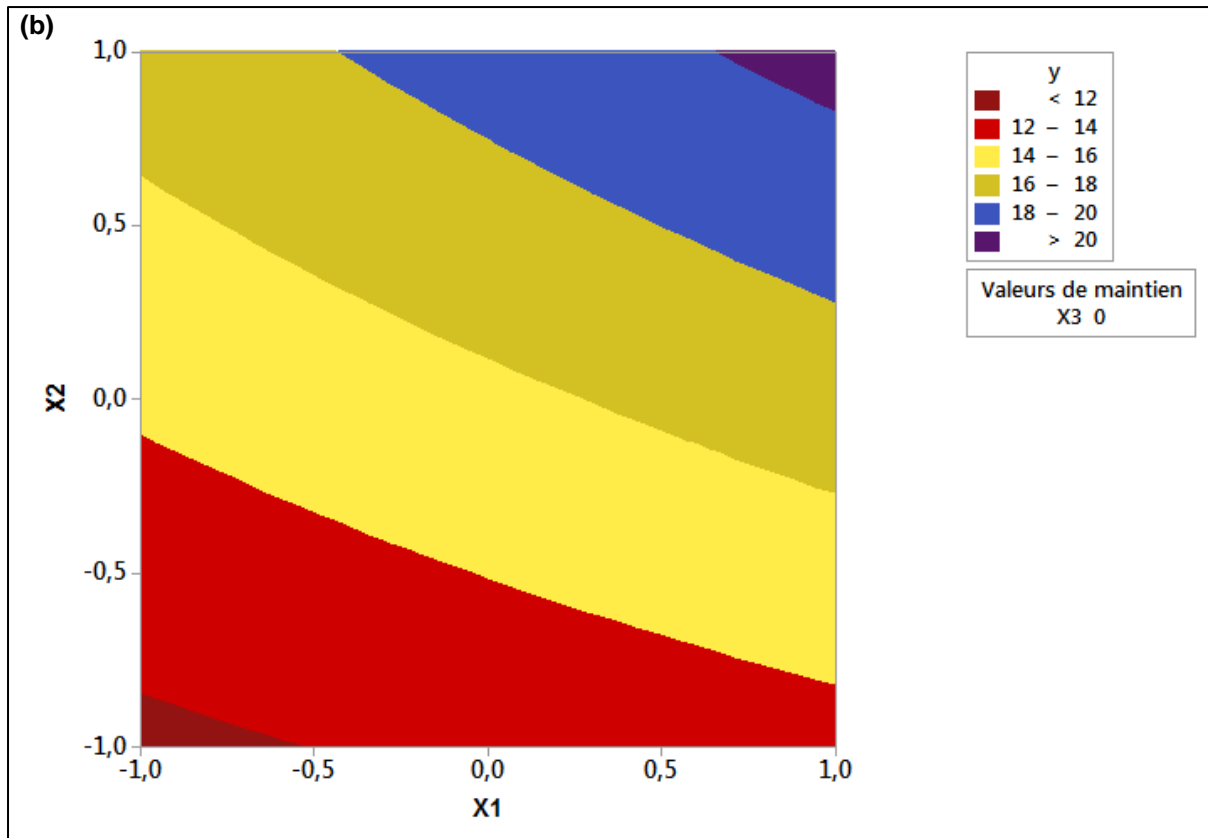


Fig.5. Contour plots exhibiting the interactive effects between two independent variables (other variables were held at their respective center levels); (a) mass percentage of glucose (X_2) and mass percentage of fructose (X_3), (b) sucrose concentration (X_1) and mass percentage of glucose (X_2), (c) sucrose concentration (X_1) and mass percentage of fructose (X_3).

IV. CONCLUSION

In this study, the sucrose solubility (thermodynamic equilibrium) has been modeled as a function of sucrose concentration and mass percentages of glucose and fructose applying the experimental design method. Predicted values obtained using the model equation were in very good agreement with the observed values ($R^2 = 0.999$). The prediction capability of the proposed model was verified by additional batch experiments conducted in the experimental area of each factor. The validation results confirm that the developed model provided a satisfactory fit to the experimental data. The results show that the presence of glucose and fructose in the mixture causes a sucrose solubility decrease.

REFERENCES

- [1.] A. Myerson, Handbook of industrial crystallization, Butterworth-Heinemann, 2002.
- [2.] B. R. Bhandari and R. W. Hartel, "Co-crystallization of sucrose at high concentration in the presence of glucose and fructose", Journal of Food Science, 2002(67), 1797.
- [3.] J. W. Mulin, Crystallization, Butterworth-Heinemann, London, 2001.
- [4.] A. Mosen, Beet-sugar handbook, Wiley, Hoboken, New Jersey, 2005.
- [5.] S. H. Yalkowsky and Y. He, P. Jain, Handbook of aqueous solubility data, CRC Press, Boca Raton, 2010.
- [6.] M. Mathlouthi and P. Reiser, Sucrose properties and applications, Springer, Dordrecht, 1995.
- [7.] J.E. Helt, "Effects of supersaturation and temperature on nucleation and crystal growth in a MSMPR crystallizer ", Retrospective Theses and Dissertations, 1976(6213).
- [8.] A. Mersmann, Crystallization technology handbook, 1st ed., New York, 1994.
- [9.] W. R. Hartel and A.V. Shastry, "Sugar crystallization in food products", Critical Reviews in Food Science & Nutrition, 1991(30), 49-112.
- [10.] A. Borji and A. Jourani, "Spectrophotometry as a method for the determination of solubility of sucrose in water and metastable zone width of its aqueous solutions", Crystal Research and Technology, 2018 (53), 6.
- [11.] K. Sangwal, Additives and crystallization processes: from fundamentals to applications, John Wiley & Sons, 2007.
- [12.] A. Borji, Fz. Borji, and A. Jourani. "Sugar Industry: Effect of Dextran Concentrations on the Sucrose Crystallization in Aqueous Solutions", Journal of Engineering, 2019(2019), 6.
- [13.] D. C. Montgomery, Design and analysis of experiments, 5th ed. New York: John Wiley & Sons, 2001.
- [14.] J. L. Goupy, Methods for experimental design, Data Handling in Science and Technology, 1993.
- [15.] L. C. Morais, O. M. Freitas, E. P. Gonçalves, L. T. Vasconcelos and C. G. Gonzalez Beça, "Reactive dyes removal from wastewaters by adsorption on Eucalyptus Bark: variables that define the process", Water Research, 1999(33), 979-988.

- [16.] S.Viénat-Nikodemski, Isolement et caractérisation des polysaccharides des jus concentrés de betterave sucrière. Thèse de Doctorat, Biotechnologie et Industrie Alimentaires, Institut National Polytechnique de Lorraine, I.N.PL, Nancy, 1994.
- [17.] K. Adinarayana and P. Ellaiah, "Response surface optimization of the critical medium components for the production of alkaline protease by a newly isolated *Bacillus* sp.", *Journal of Pharmacy & Pharmaceutical Sciences*, 2002(5), 272–278.
- [18.] R. Sen and T. Swaminathan, "Response surface modeling and optimization to elucidate and analyze the effects of inoculum age and size on surfactin production", *Biochemical Engineering Journal*, 2004(21), 141–148.
- [19.] A. Borji, Fz. Borji, and A. Jourani. "A New Method for the Determination of Sucrose Concentration in a Pure and Impure System: Spectrophotometric Method." *International journal of analytical chemistry*, 2017 (2017), 6.
- [20.] G. Vavrincz, "NeueTabelleüber die Löslichkeit reiner Saccharose in Wasser", *Zuckerindustrie*, 1962(12), 481-487.

Phosphate Industry: Gypsum Crystallization under the Industrial Conditions of Wet-Process Phosphoric Acid Production

Fatima-Ezzahra BORJI^{1,*}, Abdelali BORJI¹ and Abdelaziz JOURANI¹

¹Laboratory of Physical Chemistry of Processes and Materials, Department of Applied Chemistry and Environment
Faculty of Sciences and Techniques, University Hassan 1
Settat, Morocco

ABSTRACT

The crystallization is an important separation and purification process, governed by nucleation and growth. It is present in different industries. In the phosphoric acid manufacturing process, the crystallization of the gypsum is crucial which determines the efficiency of the filtration, and hence the quality of the acid produced. To deal with the problems related to this step, it is extremely necessary to know the solubility and the supersaturation limit curves of gypsum under industrial conditions of phosphoric acid production.

The present study investigated the effect of the phosphoric acid concentration, as well as the effects of the Mg^{2+} , Al^{3+} and Cd^{2+} ions, as impurities, on the solubility and the metastable zone width of calcium sulfate dihydrate (gypsum) under simulated conditions of wet-process phosphoric acid production using the spectrophotometric method.

The results show the decrease in the metastable zone width with the decrease of the phosphoric acid concentration in the mixture. The results also show the increase of the gypsum solubility in the presence of these impurities. It should be noted that the effect of Mg^{2+} ions is more pronounced compared to that of other impurities.

Keywords—*crystallization; gypsum; solubility; metastable zone width; impurities.*

I. INTRODUCTION

The strong growth of the world population, less than 2 billion in 1920, more than 7 billion today and about 10 billion by 2050, generates an increase in world agricultural production of 77% in order to meet the demand for food of the world population [1]. So it is imperative to increase agricultural production and this by increasing the production of fertilizers that is directly related to the production of phosphoric acid.

The production of wet-process phosphoric acid is carried out in several stages whose the sulfuric acid attack of phosphate rock is the crucial step [2]. Indeed, the mastery of this step allows the control of the different losses in phosphate, namely: unattacked losses, co-crystallized losses and filtration losses [3]. In the step of sulfuric acid attack of phosphate rock, the gypsum crystallization is an ultimate step insofar as the increase in the size of the gypsum crystals results in the increase of the efficiency of the filtration unit and consequently the increase in the productivity [4]. In fact, to have a good yield and

a good efficiency, it is necessary to master and control the thermodynamic and kinetic parameters of the gypsum precipitation, in particular the solubility and the metastable zone width. These parameters can be influenced by the impurities present in the reaction medium [5-10].

In this context, the main objective of this paper is to study the effect of phosphoric acid concentration and some impurities, unavoidably present in reaction medium (Mg^{2+} , Al^{3+} and Cd^{2+}), on the gypsum solubility and the metastable zone width.

II. EXPERIMENTAL SECTION

Pure phosphoric acid and sulfuric acid have been used to prepare the following solutions:

- Solution 1: $x\%$ P_2O_5 et $y\%$ H_2SO_4 ;

With: $x \in \{30,15\}$ and $y \in \{2.5,1.5,1\}$

- Solution 2: 20% P_2O_5 ;
- Solution 3: 40% H_2SO_4 .

250 ml of solution 1 was heated to $80^\circ C$ in a jacketed reactor using a cryothermostat. The required amount of $CaHPO_4 \cdot 2H_2O$ is dissolved in 50 ml of solution 2 with the desired mass percentage of impurity. The obtained solution from dissolving and the corresponding sulfuric acid for reaction with dicalcium phosphate dihydrate (solution 3) were added simultaneously to the heated solution. The reaction was maintained at $80^\circ C$ with constant agitation.

The absorbance of the mixture is then measured every 5 min until the sudden change in the value of the absorbance. This value corresponds to the supersaturation limit (a sample is taken to characterize the mixture at the limit of supersaturation by dosage) [11]. Then, the reaction is left for 24 hours to reach equilibrium. The slurry so formed is filtered to separate the gypsum from the saturated filtrate. The saturation concentration is determined by the filtrate titration. Fig. 1 represents the experimental setup used in this study.

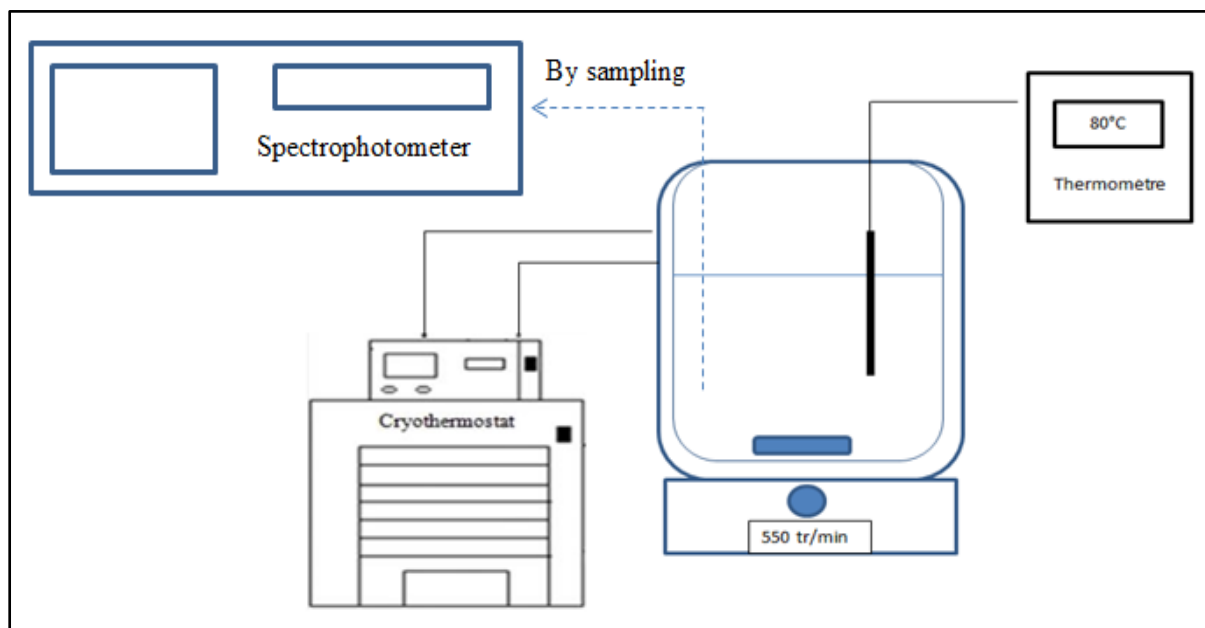


Fig. 1: Experimental setup.

III. RESULTS AND DISCUSSIONS

Increasing the yield remains the goal of all industries. In the phosphoric acid production industry, to achieve this objective, phosphate losses must be avoided or reduced. In fact, the production of wet-process phosphoric acid leads to unavoidable losses of phosphate following the precipitation of gypsum during the extraction of phosphoric acid from natural phosphate [12]. There are three types of phosphate losses, namely: unattacked losses, co-crystallized losses and a loss of phosphate that occurs during the filtration of the reaction slurry, some of the phosphoric acid produced remains trapped in the cakes of the gypsum, this type of loss can be reduced by increasing the filter size or by increasing the flow rate washing water. For the industry, changing the size of the filter or reducing the rate of production is impossible. The addition of the additional washing water remains the most adapted solution to the industry, but it costs expensive because of the insufficient storage which leads to an evacuation of the stored acid towards sewer and the increase in the energy intake used for the concentration of the acid produced. So it remains to think to improve the quality of the gypsum cake, i.e. improving the gypsum crystallization (size, shape, etc.), which improves the efficiency of the filtration unit reducing thereafter the rate of phosphate loss trapped in the gypsum cake. In this context, the experimental tests were carried out within a phosphoric acid manufacturing industry (OCP SA, Morocco). These tests concern the modification of the distribution of sulfate and calcium ions in the reaction medium. For this, the rates and the injection points of sulfuric acid and pulp have been modified. Then samples were taken from different compartments of the attack tank (see Fig. 2) and the mass percentages of Ca^{2+} and SO_4^{2-} in the different compartments have been determined. In order to visualize the crystallization state, these results have been exploited to locate the points on the saturation and supersaturation limit curves using the following equations giving by Becker [3]:

$$[\% \text{CaO}] \times [\% \text{SO}_4] = 0.83 \quad \text{saturation curve (s line)} \quad (1)$$

$$[\% \text{CaO}] \times [\% \text{SO}_4] = 1.3 \quad \text{supersaturation limit curve (ss line)} \quad (2)$$

These curves consist of 3 zones (see Fig. 3): a zone above the curve of the supersaturation limit in which the formation of calcium sulphate is spontaneous, in this case small crystals will be formed. A zone between the curves of the saturation and the supersaturation limit where the formation of gypsum crystals is performed on the gypsum crystals already existed in the medium (case of industries), so we will have a crystal growth of the gypsum crystals seeded in the reaction medium, this zone is called the metastable zone [13-15]. Finally, a zone below the saturation curve, in this zone, the calcium and sulfate ions remain in solution, no nucleation is produced.

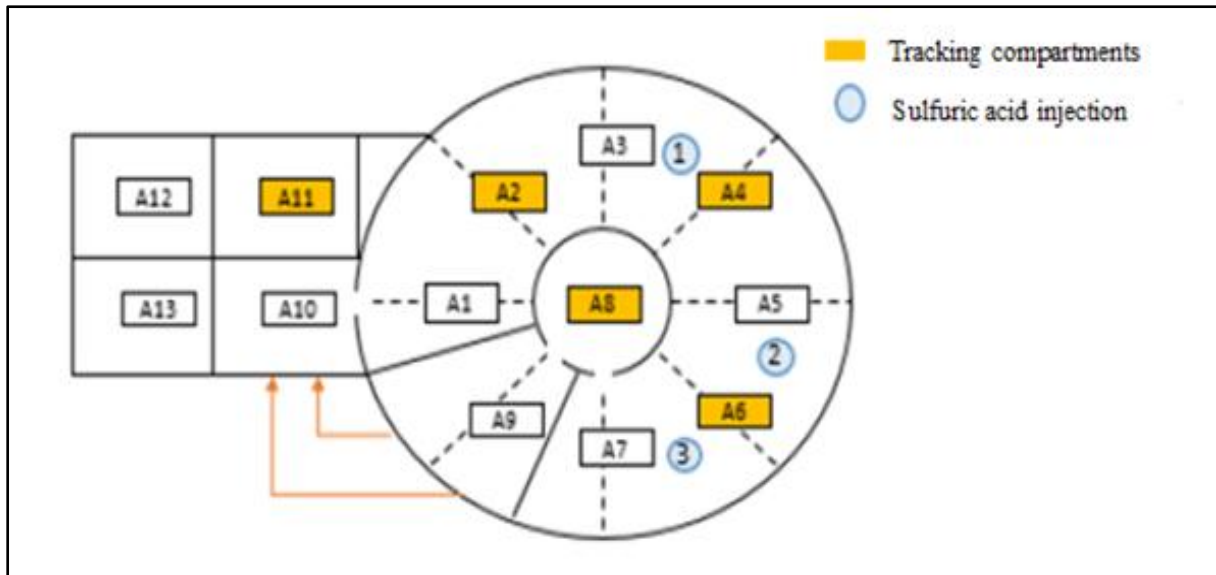


Fig. 2: Sampling points of the tank of attack.

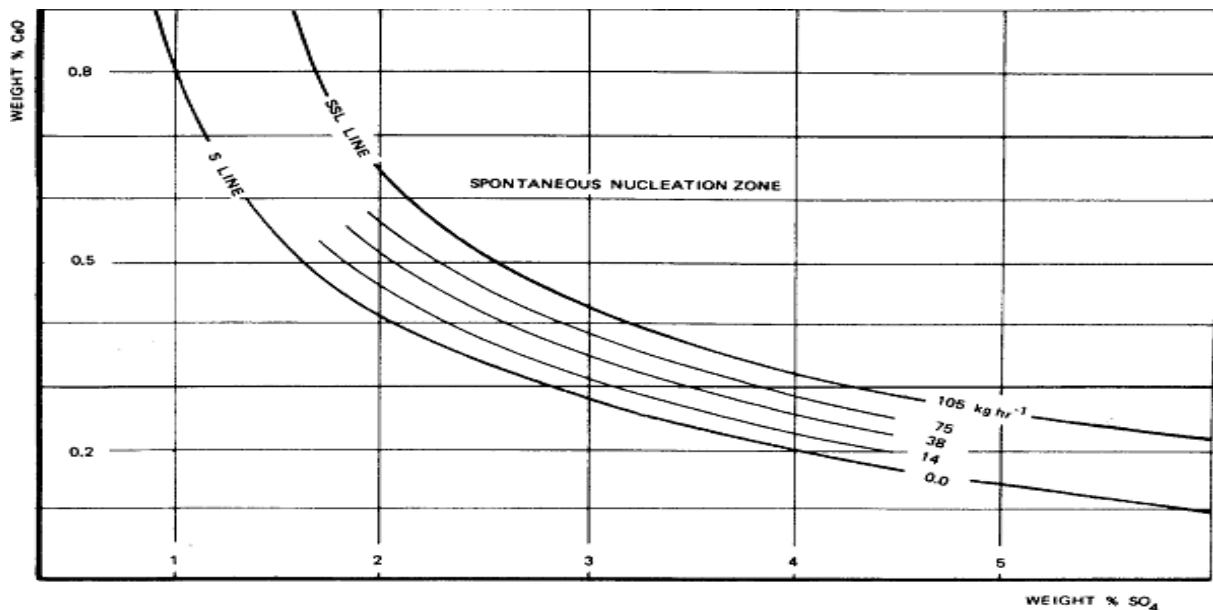


Fig. 3: Saturation and supersaturation diagram CaO/SO₄ in 30% P₂O₅ phosphoric acid at 75°C. Precipitation speed lines in kilograms of gypsum per cubic meter of slurry per hour [3].

Fig.4 represents the results obtained concerning the crystallization state of the gypsum in compartments C1, C2, C4, C6 and C8. These results show that before the modifications made, the gypsum crystallization process is not controlled because several points are outside the metastable zone (see Fig.4a). This gives rise to a spontaneous nucleation, which creates small crystals hindering subsequent filtration. After the modifications performed, all the points are in the metastable zone (see Fig.4b) which gives rise to a growth of the gypsum allowing a good filtration and consequently a good quality of the phosphoric acid produced. These results have been confirmed by the decrease in the phosphate losses as well as the increase in the concentration of the phosphoric acid produced. Figs. 5 and 6 represent the variation of the phosphoric acid concentration and the variation of the filtration losses before and after modifications, respectively.

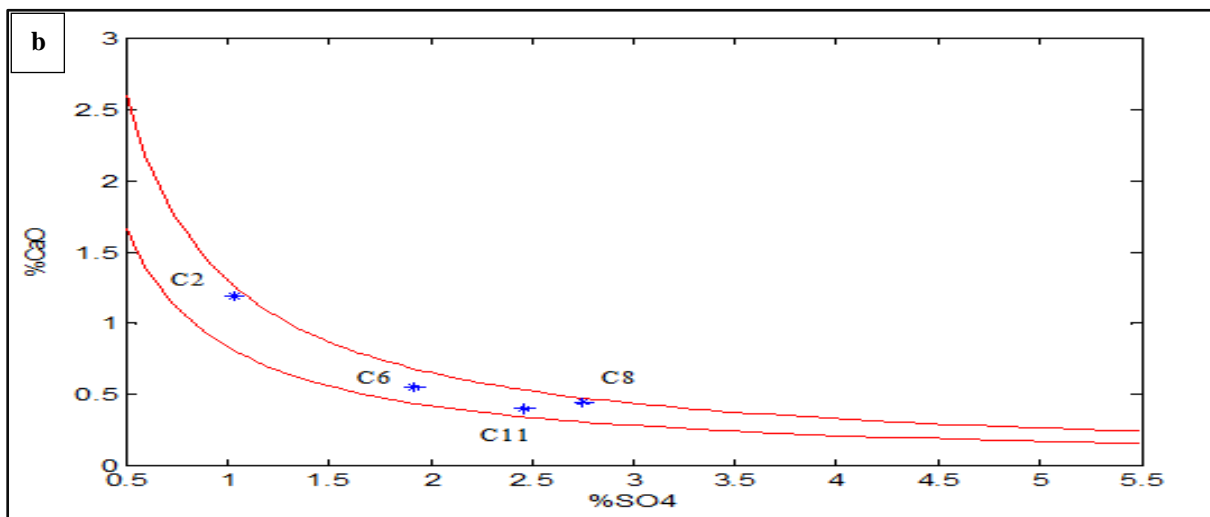
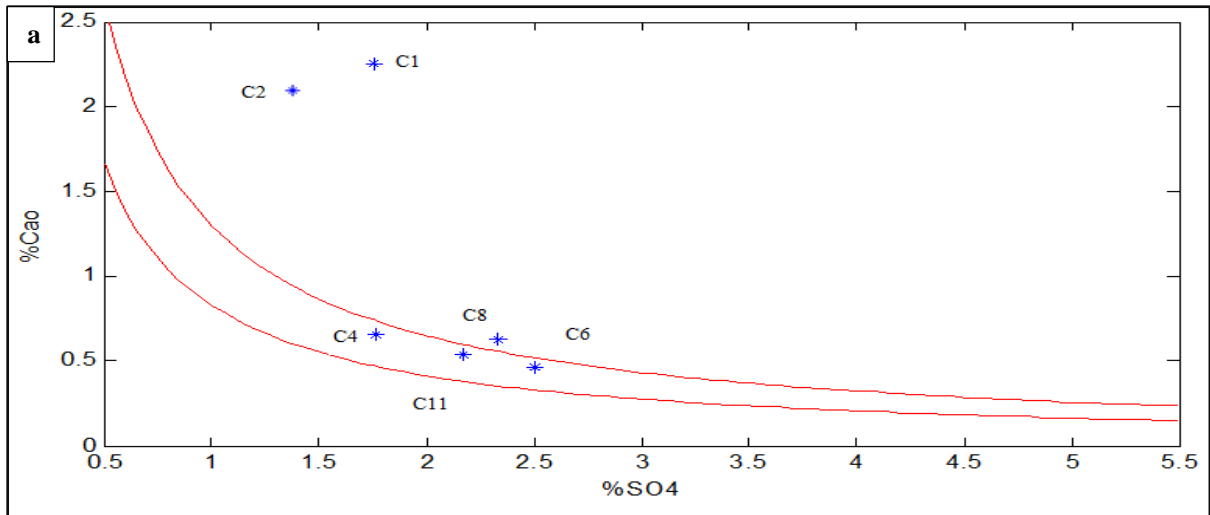


Fig. 4: Evolution of the gypsum crystallizations state before and after modifications; (a): before change of distribution of pulp and sulfuric acid in the attack tank; (b): after changing the distribution of pulp and sulfuric acid in the tank.

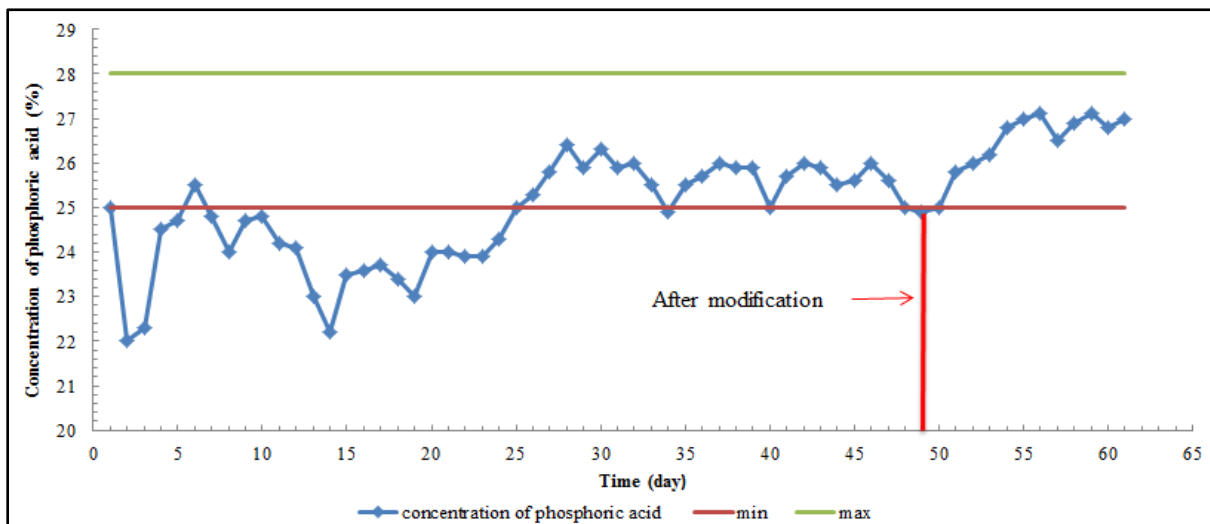


Fig. 5: Evolution of phosphoric acid concentration.

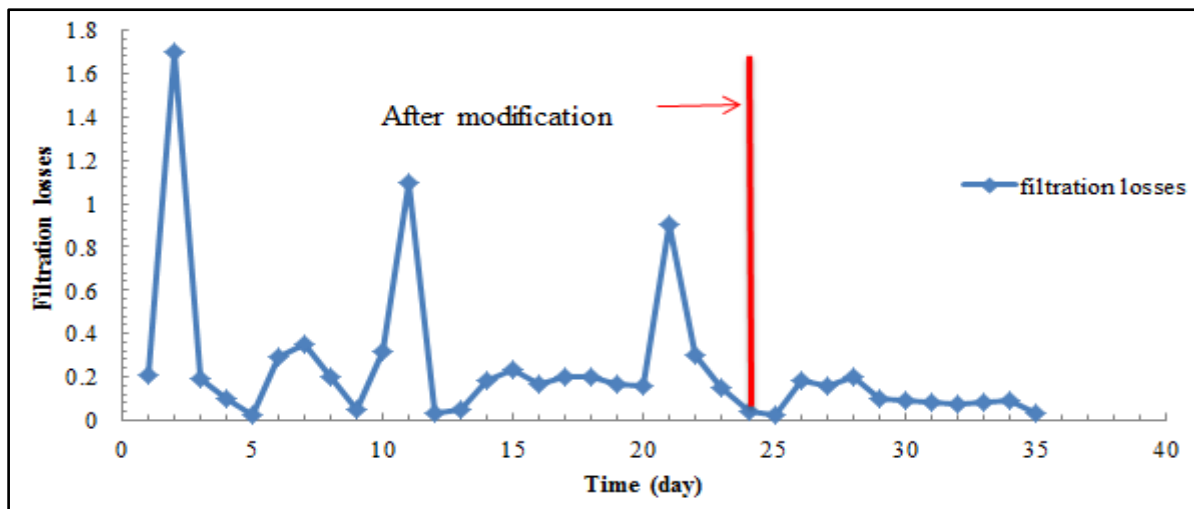


Fig.6: Evolution of filtration losses.

The results obtained show that the control of the gypsum crystallization has given rise to a good filtration. This has several advantages namely: the reduction of the filtration losses, the increase of the filtrate-slurry density and the improvement of the acid purity. All of these improvements are part of improving chemical efficiency.

From these results, it can be seen that the control of the crystallization of gypsum, in particular the solubility curves and those of the supersaturation limit under the industrial conditions of phosphoric acid production, is crucial to have a good quality of the acid produced. It should be noted that these curves strongly depend on the composition of the reaction medium such as the phosphoric acid concentration, the concentration of impurities and the sulfuric acid rate. In this context, the curves of the solubility and the metastable zone width of the gypsum crystallization have been determined as a function of phosphoric acid concentration and in the presence of Mg^{2+} , Cd^{2+} and Al^{3+} as impurities (see Figs.7, 8, 9 and 10). As can be seen from these figures, the decrease in phosphoric acid concentration in the mixture causes a gypsum metastable zone width decrease. The results also show the increase of the gypsum solubility in the presence of Mg^{2+} , Cd^{2+} and Al^{3+} . It should be noted that the effect of Mg^{2+} ions is more pronounced compared to that of other impurities.

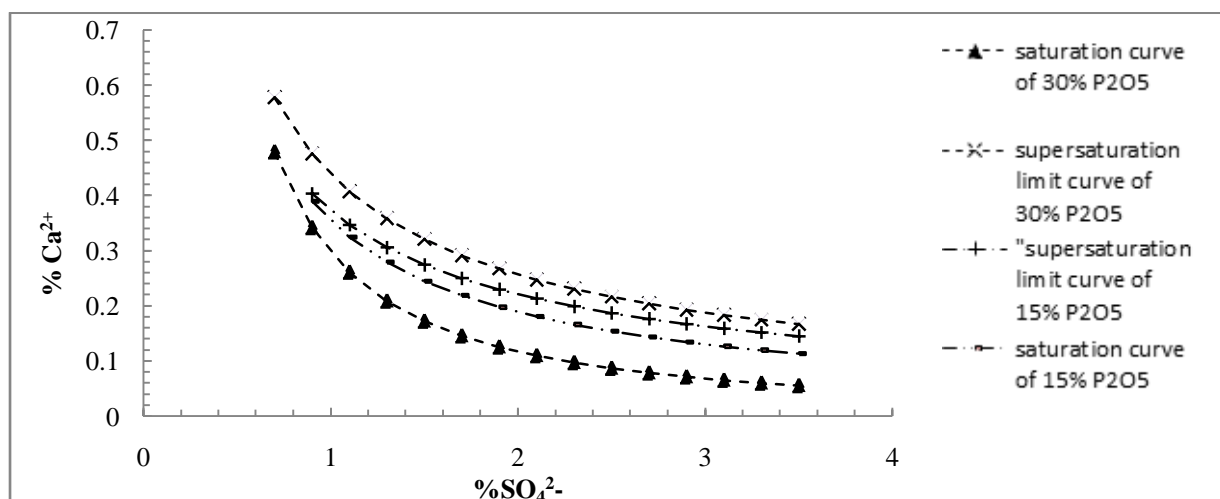


Fig.7: Effect of phosphoric acid concentration on the gypsum metastable zone width.

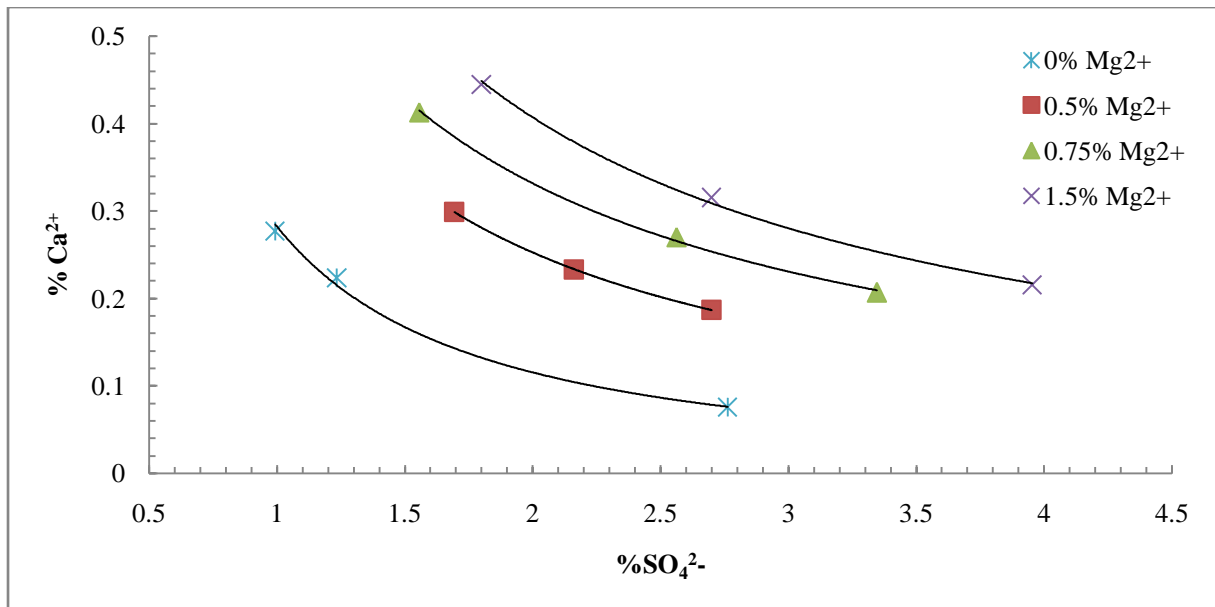


Fig.8:Effect of Mg²⁺ ions on the gypsum solubility.

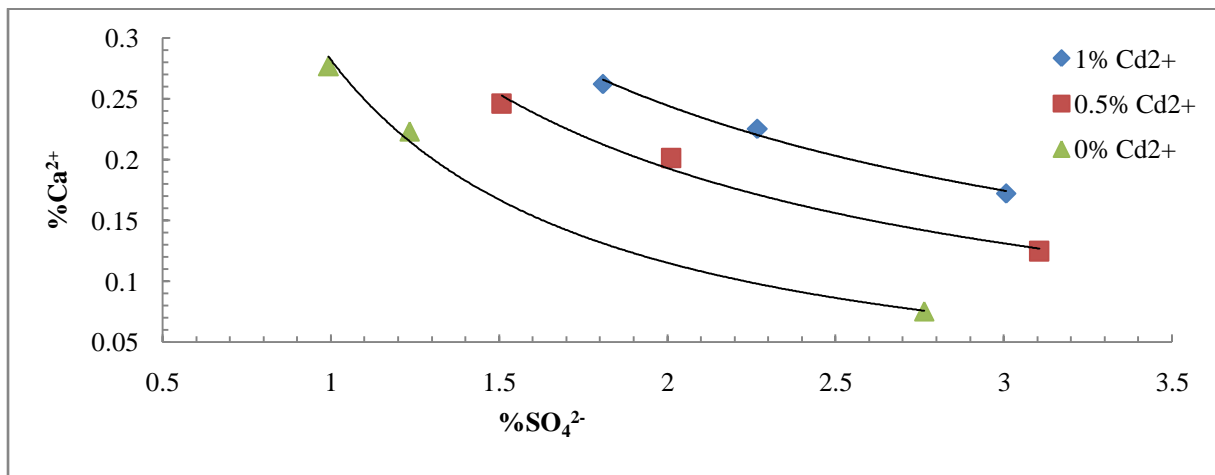


Fig.9:Effect of Cd²⁺ ions on the gypsum solubility.

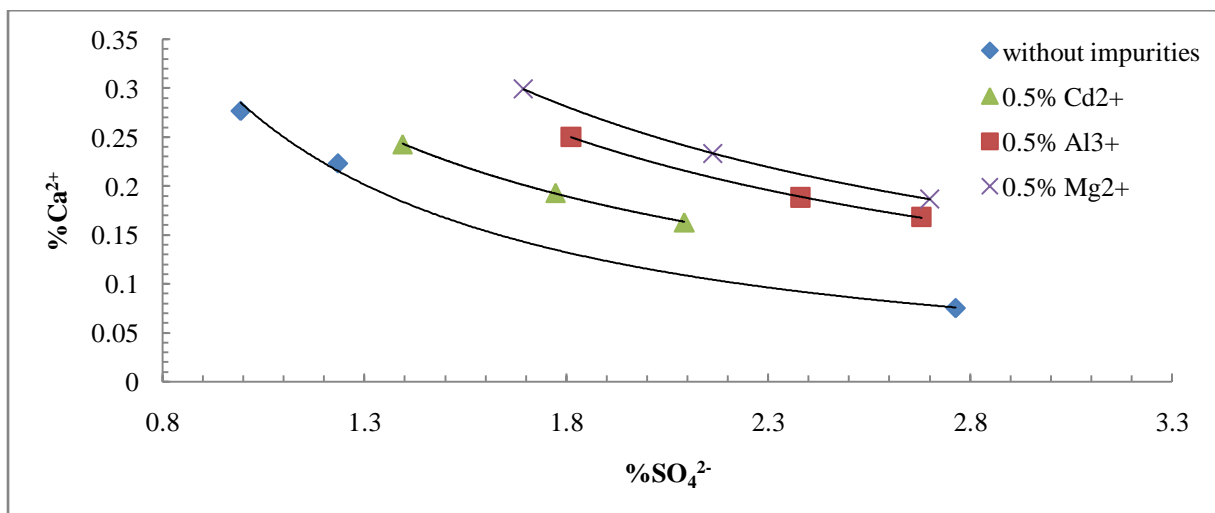


Fig.10:Effect of Mg²⁺, Al³⁺ and Cd²⁺ ions on the gypsum solubility.

IV. CONCLUSION

In this study, the gypsum crystallization under the industrial conditions of wet-process phosphoric acid production was studied. Its importance during this process has been demonstrated. The results show that the crystallization of gypsum is a crucial step to have a phosphoric acid of very good quality. The influence of the phosphoric acid concentration and impurities, such as Mg^{2+} , Al^{3+} , and Cd^{2+} , on the gypsum crystallization, in particular on the solubility and metastable zone width has been investigated using the spectrophotometric method [11]. The results show that the gypsum metastable zone width decreases when the phosphoric acid concentration decreases in the mixture. The results also show the increase of the gypsum solubility in the presence of Mg^{2+} , Cd^{2+} and Al^{3+} . It should be noted that the effect of Mg^{2+} ions is more pronounced compared to that of other impurities.

In future work, the interactions effects between these impurities on the solubility and metastable zone width of gypsum will be studied. A modeling of these two parameters as a function of phosphoric acid concentration and in impure systems will be carried out under the industrial conditions of the phosphoric acid production.

REFERENCES

- [1] J. Cooper, R. Lombardi, D. Boardman and C. Carliell-Marquet, "The future distribution and production of global phosphate rock reserves", *Resources, Conservation and Recycling* 57 (2011) 78-86.
- [2] M.M. Rashad, M.H.H. Mahmoud, I.A. Ibrahim and E.A. Abdel-Aal," Crystallization of calcium sulfate dihydrate under simulated conditions of phosphoric acid production in the presence of aluminum and magnesium ions", *Journal of Crystal Growth* 267 (2004) 372–379.
- [3] P. Becker, *Phosphates and Phosphoric Acid: Raw Materials Technology and Economics of the Wet Processes*, Marcel-Dekker, Inc., New York, 1989.
- [4] S. K. Hamdona and U. A. Al Hadad, "Crystallization of calcium sulfate dihydrate in the presence of some metal ions", *Journal of Crystal Growth* 299 (2007) 146–15.
- [5] N. Kubota, "A new interpretation of metastable zone widths measured for unseeded solutions", *Journal of Crystal Growth* 310 (2008) 629–634.
- [6] L. Yang, J. Cao and T. Luo," Effect of Mg^{2+} , Al^{3+} , and Fe^{3+} ions on crystallization of type α hemi-hydrated calcium sulfate under simulated conditions of hemi-hydrate process of phosphoric acid", *Journal of Crystal Growth* 486 (2018) 30–37.
- [7] K. Sangwal, *Additives and crystallization processes: from fundamentals to applications*, John Wiley & Sons, 2007.

- [8] A. Borji, F.E. Borji and A. Jourani, "Sugar industry: effect of dextran concentrations on the sucrose crystallization in aqueous solutions", *Journal of Engineering* 2019 (2019) 6.
- [9] H. El-shall, M. M. Rashad and E. A. Abdel-aal, "Effect of phosphonate additive on crystallization of gypsum in phosphoric and sulfuric acid medium", *Crystal Research and Technology* 37 (2002) 1264–1273
- [10] A. Myerson, *Handbook of industrial crystallization*, Butterworth-Heinemann, 2002.
- [11] A. Borji and A. Jourani, "Spectrophotometry as a method for the determination of solubility of sucrose in water and metastable zone width of its aqueous solutions", *Crystal Research and Technology* 53 (2018) 1700123.
- [12] B. Messnaoui, A. Bouhaouss and A. Derja, "A steady state model for describing the phosphate lattice loss", *Procedia Engineering* 46 (2012) 134-142.
- [13] N. Kubota, "A unified interpretation of metastable zone widths and induction times measured for seeded solutions", *Journal of Crystal Growth* 312 (2010) 548–554.
- [14] N. P. R Ajesh, C. K. LakshmanaPerumal, P. SanthanaRaghavan and P. R Amasamy, "Effect of urea on metastable zone width, induction time and nucleation parameters of ammonium dihydrogen orthophosphate" *Crystal Research and Technology* 36 (2001) 55–63.
- [15] K. Kim and A. Mersmann, "Estimation of metastable zone width in deferent nucleation processes", *Chemical Engineering Science* 56 (2001) 2315-2324.

Isolation and characterization of polycyclic aromatic hydrocarbon degrading bacteria from contaminated soil sludge in Tamilnadu

(Isolation of PAH degrading bacteria)

T. Velayutham*

*Associate Professor in Civil Engineering, FEAT, Annamalai University,

Annamalainagar – 608 002, Tamilnadu, India

ABSTRACT

Eight bacteria capable of utilizing naphthalene, as their sole source of carbon and energy for growth were isolated from contaminated soil sludge in Chidambaram, Mayiladurai, at Tamil nadu. By standard bacteriological methods, these bacteria were characterized taxonomically as belonging to the genus *Bacillus* and *Pseudomonas*. Four of the isolates (S5, S6, S2 and S3), which showed the maximum growth during screening as demonstrated by an increase in their optical densities (OD₆₁₀) and identified as *Pseudomonas* and *Bacillus* respectively, were also able to grow and degradation of naphthalene. There were visible changes in the colour of the growth medium of the isolates during their incubation, suggesting the production of different metabolites. There were also changes in their medium pH during growth. These studies demonstrate the possession by the bacterial species of novel degradative systems.

Keywords— PAHs, persistence, biodegradation, *Pseudomonas* and *Bacillus*

I. INTRODUCTION

PAHs are ubiquitous contaminants of aquatic and terrestrial ecosystems whose presence is attributable to a number of petrogenic and pyrogenic sources, which had increased since the end of the Second World War (Laflamme and Hite, 1978; NAS, 1983; Jonsen et al., 2005). Environments contaminated with PAHs are considered hazardous as studies using animals have shown the specific carcinogenic, mutagenic and teratogenic effects of some PAHs (Miller and Miller, 1974; Moore et al., 1989; Autrup, 1990). Their biochemical persistence in the environment arises from dense clouds of π -electrons on both sides of the ring structures, making them resistant to nucleophilic attack (Jonsen et al., 2005). Even though higher molecular weight PAHs such as those containing four or more benzene rings are considered to be responsible for the majority of the potential hazards of these compounds to the environment and human health (EPA, 1984), lower molecular weight types such as naphthalene (the simplest containing two benzene rings), anthracene and phenanthrene (both of which contain three benzene rings) are known to have health effects that though are comparatively mild could be potentially hazardous (Klaasen, 2001). Furthermore, some like phenanthrene is considered as a model substrate in environmental PAHs degradation studies because its structure is found in the nucleus of carcinogenic PAHs such

as benzo[a]anthracene and 3-methylcholanthrene (Cerniglia and Yang, 1984). As a result of these hazardous effects of PAHs, there is much interest in their environmental effects. Although some physical processes such as volatilization, leaching, chemical and photo oxidation are often effective in reducing the environmental level of PAHs (Bossert and Bartha, 1984; Heitkamp et al., 1988), biodegradation using microorganisms is usually the preferred and major route of PAH removal from contaminated environments because of some inherent advantages such as its cost effectiveness and more complete cleanup (Pothuluri and Cerniglia, 1994). Moreover, the physical processes are often limited to aquatic environments only. The microorganisms should possess all the necessary enzymes needed to degrade PAHs. It is known that selection or adaptation of PAH-degrading microorganisms as with other chemicals occur as a result of their previous exposure to these substances in the environment (Lewis et al., 1984; Spain et al., 1980). However, these adaptations occur slowly, and usually depend on the recalcitrance or biodegradability of the particular substance involved (Spain et al., 1980). This is especially so considering that PAHs usually have low aqueous solubility and thus, are poorly available (low bioavailability) for microbial utilization. (Jonsen et al., 2005). A lot of isolated microorganisms have been successfully utilized in major hazardous waste clean-up processes, as for example, in industrial process streams and effluents (Levinson et al., 1994). Unfortunately, most of these studies were carried out in Western countries, and to a limited extent in South America and Asia (Kiyohara et al., 1982; Ghoshal et al., 1996; Prantera et al., 2002). In this work, we report the isolation and characterization of PAH (naphthalene)-degrading bacteria from soil sediments in Tamil Nadu coastal environment, and their course of growth in naphthalene and other aromatic compounds..

II. Materials and Methods

Sample Collection

Sludge sample was collected with a sterile scoop from a layer 0 to 30 cm deep at contaminated soil sludge in Chidambaram, Mayiladudurai, Tamil Nadu, India. The sample was kept in a sterile container and stored in laboratory at 4°C (Refrigerator).

Bacterial Enrichment

Sludge sample of 10.0 g was put in to 250 ml Erlenmeyer flask having 150 ml of mineral salt broth (MSM) supplemented with 0.0250 g/l naphthalene as the single source of carbon and energy. Mineral salt medium (MSM) used was composed of (NH₄)₂SO₄ -1 g/l, KH₂PO₄ -0.2 g/l, K₂HPO₄ -1.6 g/l, MgSO₄·7H₂O -0.2 g/l, NaCl -0.1 g/l, FeSO₄ -0.1 g/l and CaCl₂·2H₂O -0.02 g/l (Sakata et al. 2004). Medium was prepared in deionized water and pH was maintained to 7-7.2 using 0.4M HCl or 0.4M NaOH. Medium was sterilized and kept at temperature 31±2°C in an orbital shaker at 120 rpm for 7 days. Afterwards, 1.0 mL sample was taken from each culture and transferred into fresh enrichment medium, followed by incubation as described above for one week. The enrichment procedure was repeated for the third time, before their bacterial contents were isolated using a solid medium containing the enrichment medium and 15.0 g/L of pure agar. Inoculated plates were purified by repeatedly sub culturing. Pure cultures obtained by this procedure were stored in slants of enrichment medium with 15.0 g/L pure agar, and also in nutrient agar, and stored at 4 °C.

Screening of the isolates for the ability to use Naphthalene as sole source of carbon for growth

A loopful of each isolate was inoculated into large test tubes containing 25 mL of screening medium. The screening medium was the same as the enrichment medium, except that 15 mg of naphthalene dissolved in DMSO was added to each tube after autoclaving, as sole source of carbon. Thereafter, the test tubes were statistically incubated by keeping on the laboratory bench at room temperature (30 – 32 °C) for three days. The

ability of each isolate to utilize naphthalene was indicated by an increase in turbidity of the medium measured at 610 nm using a UV spectrophotometer.

Identification, characterization and standardization of isolates

The isolates were identified by colour, morphological, physiological, utilization of carbon and biochemical tests were tested in our laboratory as per Bergey's manual of systematic bacteriology. All isolated bacteria were scrutinized by Gram's staining reaction to differentiate between Gram positive and Gram negative bacteria. All the isolates were code-named and subsequently used for further studies. Before usage in subsequent works, cells were washed and standardized to the McFarland nephelometer standard of 0.5 (Baron and Finegold, 1990). In all cases, 10⁸ v/v of standardized inoculum was used according to the volume of medium used. Isolates, which gave the highest OD readings, were identified to their species level.

Batch experiment of naphthalene degradation

For biodegradation studies, bacterial strains were pre-inoculated into 100 ml of MSM containing 50 mg/l Naphthalene in Erlenmeyer flasks, and incubated for 24 h at room temperature, while shaking at 120 rpm in dark. From that medium the bacterial cells were harvested and diluted in sterile medium. Then, 3 ml of bacterial cell suspension of 0.06 optical densities (OD) at 610 nm were utilized as inoculums. All batch experiments conducted in 250 ml conical flasks containing 150 ml of (MSM) at pH-8-8.5 and added naphthalene as a substrate at concentration (100 mg l⁻¹) individually as carbon source against respective uninoculated controls. The batch reactors were placed in a shaker (120 rpm) at lab temperature of 31±1°C. The growth was examined over a period of 1 day by quantifying the OD values and biomass dry weight (DW). All the operations were done under sterilized conditions and testing was conducted in triplicate. The residual PAHs were determined by gas chromatography.

III. Results and Discussions

Screening and characterization of the isolates

Twenty-eight bacterial isolates were obtained from mixed soil sludge samples after screening. Eight microorganisms were found to degrade naphthalene in mineral salt broth medium (MSM) supplemented with 25 mg/L naphthalene, as the single source of carbon and energy. The pure cultures isolated were labelled sequentially as S1, S2, S3, S4, S5, S6, S7 and S8. The microbes were characterized based on Gram staining test and cell morphology. Among them two (S1, S2, S4 and S6) were Gram negative and long, slender rods, others were Gram positive (S3, S5, S7 and S8). Each strain was further evaluated through batch experiments for its ability to degrade PAHs. From the “Fig. 1” present the growth form of the isolates observed in the occurrence of PAHs. Out of eight, four organisms S2, S3, S5 and S6 exhibited growth by utilizing PAHs in the order of S6>S5>S3>S2. The isolates S2, S3, S5 and S6 were further isolated with high purity by repeated inoculation in PAH-spiked media and plating them on petri plates. The morphological, physiological, and biochemical characteristics of these two microorganisms were tested as per the Bergey's Manual of Determinative Bacteriology (reference) and the results are summarized in Table 1 and Table 2.

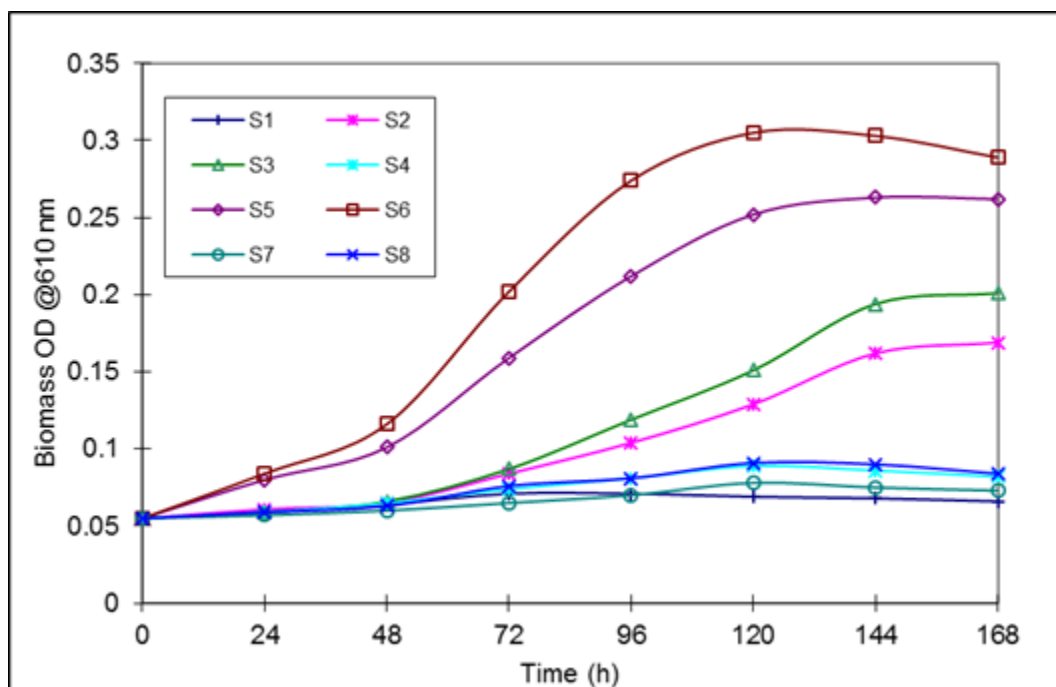


Fig. 1. Growth pattern of isolates in the presence of PAH mixtures

TABLE 1. Biochemical characteristics of the isolates

S. No	Biochemical characteristic	S2	S3	S5	S6
1	Catalase	+	+	+	+
2	Oxidase	+	+	+	+
3	Starchhydrolysis	+	+	+	+
4	Gelatinliquefaction	+	+	-	+
5	Citrate utilization	-	-	-	+
6	Denitrification	+	+	+	+
7	D-Glucose	+	+	+	+
8	Fructose	-	+	+	+
9	Gluconate	+	+	+	+
10	Glycerol	+	+	+	-
11	Tartrate	-	-	-	+
12	Malate	-	-	+	-
13	Mannitol	+	-	-	+
14	Pyruvate	-	-	+	+

TABLE 2. Morphological characteristics of the isolates

S.No.	Morphological characteristics	S2	S3	S5	S6
1	Type of colony	Small smooth convex and grey	Large opaque, adherent irregular edges	Wrinkled	Smooth
2	Cell diameter	0.5-1 μm	0.1-0.3 μm	0.7 – 0.8 μm	Less than 1.0 μm
3	Endospore	-	+	-	+
4	Pigmentation	-	-	Pale orange	-
5	Motility	+	+	+	+
6	Gram nature	Gram positive rods	Gram positive rods	Gram negative rods	Gram negative long rods

Morphologically the strain S2 and S3 were observed as rod-shaped, Gram-positive, alkaline tolerant bacterium. Optimal growth of the isolate occurred around 30°C, but growth was also observed at much normal pH (7.0-7.5). The results of bacteriological and biochemical characteristics of this organism suggested that the strain S2 and S3 belong to the genus *Bacillus*. Morphological examinations of S5 and S6 revealed that the isolate was aerobic rod-shaped, gram negative bacteria. Colonies were wrinkled and smooth, Pale orange. The results of bacteriological and biochemical characteristics of this organism suggested that the strain S5 and S6 were belongs to the genus *Pseudomonas* and *Bacillus*.

Biodegradation of Polycyclic Aromatic Hydrocarbons

The naphthalene biodegradation efficiency of isolates was studied by the initial quantity of naphthalene spiked in the media. The efficiency of PAHs removal for naphthalene concentration by the isolates in batch studies as presented in "Fig. 2". It is observed that the isolates (S6, S5, S3 and S2) were degraded naphthalene about 95.1, 42.67, 26.45 and 18.45% at 100 mg l⁻¹ initial concentration within 168h respectively. The increase in cell biomass against time for various initial naphthalene concentrations of isolates (S6, S5, S3 and S2) were presented in "Fig. 3".

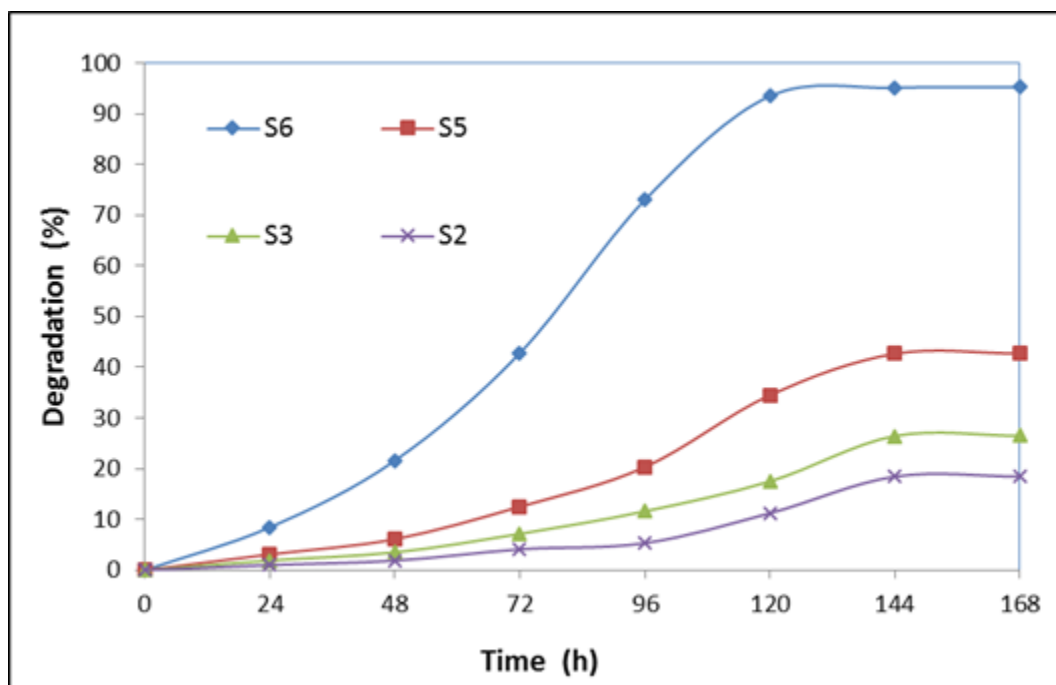


Fig. 2. Efficiency of naphthalene removal by isolates (S2,S3,S5 and S6)

PAHs are a complex class of organic compounds present in the environment. Bio degradation of PAHs by native microorganism is considered a safe and eco- friendly method to remove the contaminants. Soil contaminated with hydrocarbons are good sources for the isolation of PAHs degrading bacteria, (Jacques et al. 2009; Al-Thani et al. 2009) which can then be used for the removal of such compounds from the contaminated place. In this study, the bacterial strain was isolated from the marine sediment to utilize polycyclic hydrocarbons as single carbon energy source. Among the eight selected bacterial strains four (S2,S3,S5, and S6), showed high biomass growth in naphthalene as a sole Carbon energy. The selected four bacteria were recognized as; Bacillus and Pseudomonas. Previously different strains of Bacillus have been find out from PAHs contaminated soil (Das and Mukherjee, 2007; Jacques et al. 2009; Lin et al. 2010), which have the possible to biodegrade and utilize organic compounds. The present study the isolates(S6,S5,S3and S2) degrades naphthalene at 100 mg^l⁻¹ within 168 h were 95.1,42.67,26.45 and 18.45%.

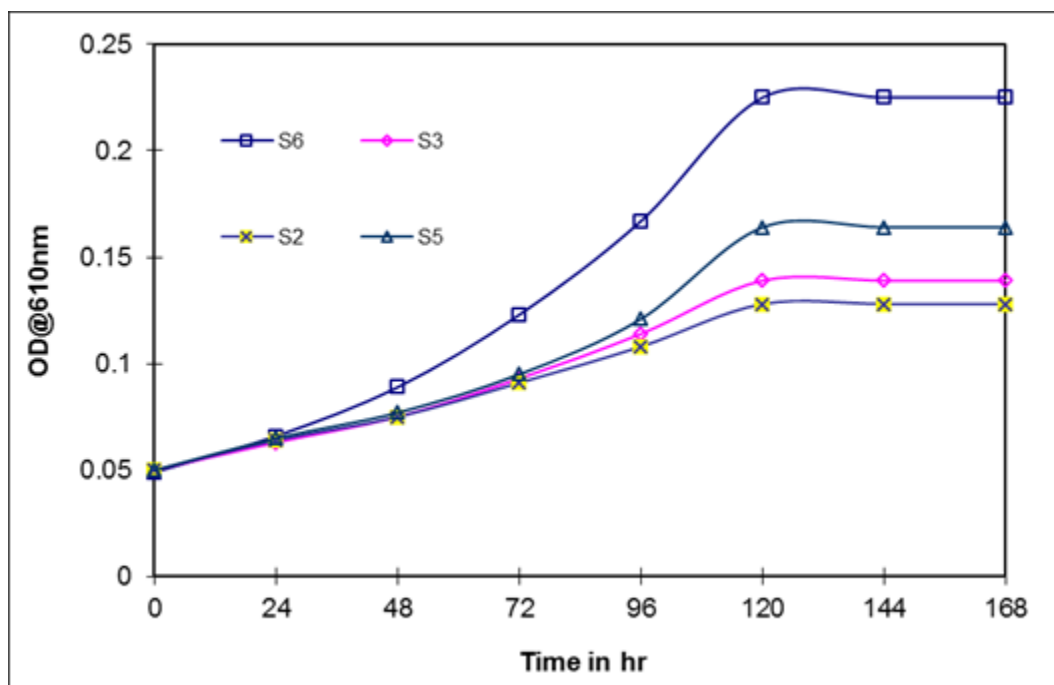


Fig. 3. Effect of naphthalene concentration (100 mg l^{-1}) on growth of isolates (S2,S3,S5 and S6)

Conclusions

In the present study, we conclude the degradation efficiency of (PAH) by isolated aerobic bacteria(S2,S3,S5 and S6) was performed. The PAHs degradation tests were led in liquid medium, with the concentration of naphthalene (100 mg l^{-1}).The results exposed that the bacteria(S6) removed naphthalene completely 95.15 % at 168 h. Based on the results, the biodegradation potential of bacteria isolated from sludge should further be examined and optimized for bioremediation purpose. In future more studies on the interaction between different microorganisms, mixtures of PAHs, and effects of different environmental factors on biodegradation are essential

References

- [1.] Arulazhagan.P. N. & Vasudevan b., 2011, Biodegradation of polycyclic aromatic hydrocarbons by a halotolerant bacterial strain Ochrobactrum sp. VA1 Marine Pollution Bulletin 62 388–394
- [2.] Autrup, H., (1990)., Carcinogen metabolism in cultured human tissues and cells. Carcinogen., 11, 707-712.
- [3.] Banerjee, D. K., P. M. Fedorak, A. Hashimoto, J. H. Masliyah, M. A. Pickard, and M. R. Gray. 1995.
- [4.] Monitoring the biological treatment of anthracene-contaminated soil in a rotating-drum bioreactor. Appl.Microbiol. Biotechnol. 43:521-528
- [5.] Bauer, J. E. and Capone, D. G., (1985). Degradation and mineralization of the polycyclic aromatic hydrocarbons anthracene and naphthalene in inter tidal marine sediments. Appl. and Environ. Microbiol., 50, 81-90.
- [6.] Bosch, R., Garcia-Valdes, E. and Moore, E. R. B., (2000). Complete nucleotide sequence and evolutionary significance of a chromosomally encoded naphthalene-degradation lower pathway from Pseudomonas stutzeri AN 10. Gene., 245, 65-74.
- [7.] Boyd, D. R., N. D. Sharma, F. Hempenstall, M. A. Kennedy, J. F. Malone, C. C. R. Allen, S. M. Resnick, and D. T. Gibson. 1999. bis-cis-Dihydrodiols: a new class of metabolites from biphenyl dioxygenase catalyzed sequential asymmetric cis-dihydroxylation of polycyclic arenes and heteroarenes. J. Org. Chem.64:4005-4011
- [8.] Churchill, S. A., J. P. Harper, and P. F. Churchill. 1999. Isolation and characterization of a Mycobacterium species capable of degrading three- and four-ring aromatic and aliphatic hydrocarbons. Appl. Environ. Microbiol. 65:549-552

- [9.] Cerniglia, C. E., (1984). Microbial transformation of polycyclic aromatic hydrocarbons. *Adv. In Appl. Microbiol.*, 30, 31- 71.
- [10.] Cerniglia, C. E., and Yang, S. K., (1984). Stereoselective metabolism of anthracene and phenanthrene by the fungus *Cunninghamella elegans*. *Appl. Environ. Microbiol.*, 47, 119-124.
- [11.] Fu, C., Pfanstiel, S., Gao, C., Yan, X., Govind, R. and Tabak, H., (1996). Studies on Contaminant biodegradation in slurry, water and compacted soil tube reactor. *Environ. Sci. Technol.*, 30, 743-750.
- [12.] Ghoshal, S., Ramaswami, A. and Luthy, R. G., (1996). Biodegradation of naphthalene from coal tar and heptamethylnonane in mixed batch systems. *Environ. Sci. Technol.*, 30, 1282 – 1291.
- [13.] Heitkamp, M. A., Freeman, J. P. and Cerniglia, C. E., (1987). Naphthalene biodegradation in environmental microcosms: estimates of degradation rates and characterization metabolites. *Appl. And Environ. Microbiol.*, 53, 129-136.
- [14.] Heitkamp, M. A., Franklin, W. and Cerniglia, C. E., (1988). Microbial metabolism of polycyclic aromatic compounds: isolation and characterization of a pyrene-degrading bacterium. *Appl. Environ. Microbiol.*, 54, 2549-2555.
- [15.] hibault, S. L., M. Anderson, and W. T. Frankenberger, Jr. 1996. Influence of surfactants on pyrene desorption and degradation in soils. *Appl. Environ. Microbiol.* 62:283-287
- [16.] Holman, H.-Y. N., Y. W. Tsang, and W. R. Holman. 1999. Mineralization of sparsely water-soluble polycyclic aromatic hydrocarbons in a water table fluctuation zone. *Environ. Sci. Technol.* 33:1819-1824
- [17.] Jonsen, A. R., Winding, A., Karlson, U. and Roslev, P., (2002). Linking of microorganisms to phenanthrene metabolism in soil by analysis of ¹³C-labelled cell-lipids. *Appl. Environ. Microbiol.*, 68, 6106-6113.
- [18.] Jonsen, R. J. and Karlson, U., (2004). Evaluation of bacterial strategies to promote the bioavailability of polycyclic aromatic hydrocarbons (PAHs). *Appl. Microbiol. Biot.*, 63, 452-459.
- [19.] Jonsen, R. J., Lucas, Y. W. and Harms, H., (2005). Principles of microbial PAH-degradation in soil. *Environ. Poll.*, 133, 71-84.
- [20.] Kastner, M., Breuer-Jammali, M. and Mahro, B., (1994). Enumeration and characterisation of the soil microflora from hydrocarbon-contaminated soil sites able to mineralise polycyclic hydrocarbons (PAH). *Appl. Microbiol. Biotechnol.*, 41, 267-273.
- [21.] Kiyohara, H. K., Nagao, K., Kuono, K. and K. Yano., (1982). Phenanthrene-degrading phenotype of *Alkaligenes fecalis* AFK2. *Appl. Environ. Microbiol.*, 43, 458-461.
- [22.] Laflamme, R. E., and Hite, R. A., (1978). The global distribution of polycyclic aromatic hydrocarbons in recent sediments. *Geochim. Cosmochim. Acta.*, 42, 289-303.
- [23.] Lewis, D. L., Hodson, R. E. and Freeman. L. F., (1984). Effects of microbial community interactions on transformation rates of xenobiotic chemicals. *Appl. Environ. Microbiol.*, 48, 561-565.
- [24.] Mueller, J. G., Chapman, P. J., Blattman, B. O. and Pritchard, P. H. (1990). Isolation and characterization of a fluorantheneutilizing strain of *Pseudomonas paucimobilis*. *Appl. Environ. Microbiol.*, 56, 1079-1086.
- [25.] Meyer, S., R. Moser, A. Neef, U. Stahl, and P. Kampfer. 1999. Differential detection of key enzymes of polyaromatic-hydrocarbon-degrading bacteria using PCR and gene probes. *Microbiology* 145:1731-1741
- [26.] Pranter, M. T., Drozdowicz, A., Leite S. G. and Rosado A. S., (2002). Degradation of gasoline aromatic hydrocarbons by two N₂-fixing soil bacteria. *Biotechnol. Lett.*, 24, 85-89.
- [27.] Renner, R. 1999. EPA to strengthen persistent, bioaccumulative, and toxic pollutant controls mercury first to be targeted. *Environ. Sci. Technol.* 33:62.
- [28.] Schneider, J., R. Grosser, K. Jayasimhulu, W. Xue, and D. Warshawsky. 1996. Degradation of pyrene, benz[a]anthracene, and benzo[a]pyrene by *Mycobacterium* sp. strain RJGII-135, isolated from a former coal gasification site. *Appl. Environ. Microbiol.* 62:13-19
- [29.] Wang, R.-F., A. Luneau, W.-W. Cao, and C. E. Cerniglia. 1996. PCR detection of polycyclic aromatic hydrocarbon-degrading mycobacteria. *Environ. Sci. Technol.* 30:307-311
- [30.] Zeng, E. Y., and C. L. Vista. 1997. Organic pollutants in the coastal environment off San Diego, California. 1. Source identification and assessment by compositional indices of polycyclic aromatic hydrocarbons. *Environ. Toxicol. Chem.* 16:179-188

Design of Mobile Meteorological Station with Embedded System Control

Ahmet Kayabasi, Berat Yildiz, Kadir Sabanci, Abdurrahim Toktaş, Mehmet Yerlikaya

Department of Electrical and Electronics Engineering, Engineering Faculty
Karamanoglu Mehmetbey University, 70100, Karaman, Turkey

ABSTRACT

Meteorological events have become an indispensable part of our daily life. The estimation/analysis of the meteorological data helps us to put our daily work on the track. Thanks to weather forecasts made by meteorological stations, we take precautions in many areas of our lives and prevent weather events from adversely affecting our lives. In this study, a mobile meteorological station was designed by using Arduino embedded system control board. Meteorological parameters such as temperature/humidity, pressure and wind parameters were measured with Arduino Mega 2560 control card, momentarily. Firstly, the measurement of meteorological parameters was carried out separately to each other. After stable and appropriate measurements were observed by making individual measurements, all measurements in the established meteorological station were combined and recorded. The designed intelligent system was utilized for the measurement in the field of Engineering Faculty at the Karamanoğlu Mehmetbey University, Yunus Emre Campus. The results obtained with the designed mobile meteorological station show that the system can be successfully used to measure the weather conditions.

Keywords—*Meteorology, Meteorological Station, Embedded System, Arduino*

I. INTRODUCTION

The environmental conditions of the habitats in which they live are vital for the survival of living forms on earth. The most important factors in these environmental conditions are the meteorological data that determine the weather conditions. Therefore, weather forecasting is based on meteorological data. Meteorology, examining all the events and changes occurring in the atmosphere surrounding the earth, is also a science that explores the consequences of living things and the world as a result of these events and changes [1]. Meteorological stations are mechanical and electronic units for this purpose. These units are mainly composed of the central control unit, sensors, memory unit and visualization unit [2]. Thanks to these stations, a system that can detect and process weather events and changes can be created. Obtaining these meteorological data will make it easier to take precaution against the negative impacts on the habitats of living things and even minimize the harm that will be experienced. According to climate scientists, the air is dependent on changing processes in the atmosphere and covers all of the atmospheric events at any place on earth or at any time [3]. Therefore, many parameters such as temperature, rains, humidity, wind, pressure, and evaporation in any part of the earth play an important role in determining the instantaneous state of the atmosphere. These

momentary situations that occur in the atmosphere have a significant effect on human life. Many events in human life are shaped and changed depending on weather events [4]. Therefore, considering these factors, making short-term or long-term forecasts is very important for human life. Weather condition is effective in many areas such as transportation, safety, health, food, and energy production in human life. Its effects can spread over a wide area and can be affected very quickly. So, changes in weather events are important for every minute of human life. For this, when meteorological data are collected, the variables that affect the course of the weather condition must be accurately identified and measured. By means of real-time meteorological weather measurements and data obtained by geographic information systems, prewarning and precautionary systems against weather events can be developed. In order to obtain meteorological data, many methods have been developed using these units. In an automatic weather station (AWS) design, data collection and processing processes were carried out at the station equipped with flexible and high-performance software and long-lasting devices. The remote control can also be provided for changes in this system [5].

In this study, an intelligent meteorological station with a mobile platform was tried to be established in order to determine the weather conditions of the Engineering Faculty of Karamanoğlu Mehmetbey University. The control of the produced station was made via the embedded system on the mobile platform. Temperature, humidity, pressure and wind sensors in the system are measured and stored on the Arduino embedded system board.

II. DESIGN OF PORTABLE METEOROLOGICAL STATION

A mobile and intelligent meteorological station was designed to observe the factors affecting the weather conditions such as temperature, humidity, pressure and wind speeds in the Karamanoğlu Mehmetbey University Yunus Emre Campus. The block diagram in Fig. 1 was performed and recorded in the meteorological station.

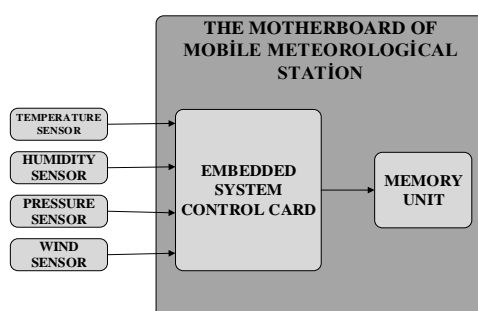


Fig.1. Block diagram of Mobile Meteorological Station design

A. Embedded System Control Board

The Arduino Mega 2560 embedded system control card, as shown in Fig. 2, was used as the control unit in the mobile meteorological station. It is an Arduino card based on ATmega2560 and has 54 digital input/output pins. 14 of them can be used as a PWM output. There are also 16 analog inputs, 4 UART (serial ports), 16 MHz Crystal Oscillator, USB connection, adapter input, ICSP output, and a Reset button. The Arduino Mega 2560 can be powered by a USB and an external adapter or battery. The power supply is automatically selected. The optimum supply voltage range of the card is between

7-12V. The unique feature of the Arduino Mega2560 from other cards is that the FTDI USB-to-serial drive connector is not used. The USB-to-Serial connector is programmed as an ATmega16U2 USB-to-serial converter. All 54 digital I/O pins operate at 5 volts and can be used as input or output using pin Mode (), digital Write (), and digital Read () functions. Each pin provides a maximum of 40mA input or output current. Pins have 20-50 kOhm pull-up resistors (normally disconnected). Each Mega 2560 has 16 analog inputs in 10-bit resolution. By default, it operates in the range 0-5V, but the reference voltage range can be changed with the AREF pin and analog Reference () function.

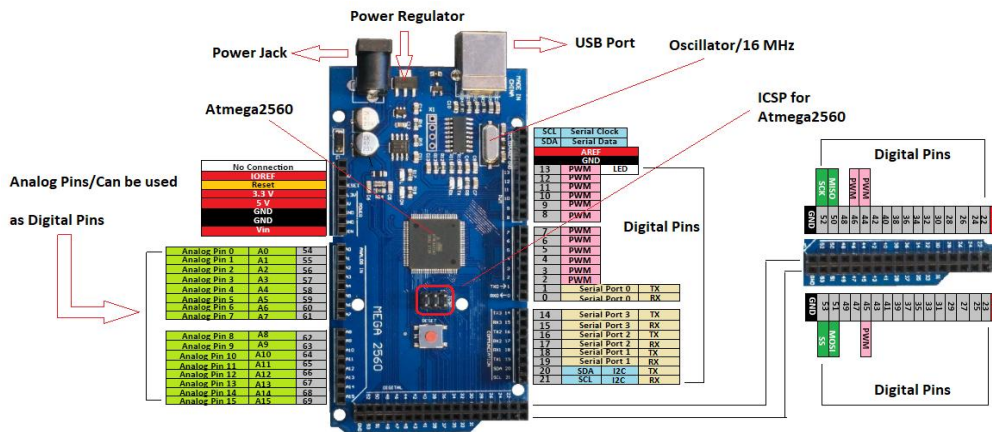


Fig. 2. Overview of the Arduino Mega 2560 [6].

The card is programmed via ArduinoIDE. The bootloader comes on a piece of code to install software on the card. You can also skip the bootloader and program the microcontroller directly via ICSP. It also has USBovercurrent protection. Normally, each computer has this protection, but the Mega2560 also has a fuse that blows out if more than 500mA of current is applied. These features are briefly summarized in Table 1.

TABLE I. FEATURES OF THE ARDUINO MEGA 2560

Microcontroller	ATmega2560
Operating voltage	5V
Supply Voltage (Limit) / (Recommended)	6-20V / 7-12V
Digital I / O Pins	54 (14 in PWM output)
Analog Input Pins	16
Current of I / O Pins	40 mA
3.3V Pin current	50 mA
Flash Drive	256 KB (uses 8kB of bootloader)
SRAM	8 KB
EEPROM	4 KB
Clock Frequency	16 MHz

B. Temperature/Humidity Measurement

For the measurement of temperature and humidity, the DHT22 temperature and humidity sensor, which is shown in Fig. 3, is used. DHT sensors consist of two parts: a capacitive humidity sensor and thermistor. The DHT22 temperature and humidity sensor is an advanced sensor unit that provides

calibrated digital signal output. The operating voltage is between 3,3 and 5 V. It has high reliability and stable structure in long term studies. With 8-bit microprocessor, it can respond quickly and accurately. It can measure the temperature with an error margin of +/- 1° C between -40-80° C and can measure the humidity with an error margin of +/- 5%RH between 0-100% RH. Depending on the data collection period of the sensor, measurement results can be taken in 2 second periods.

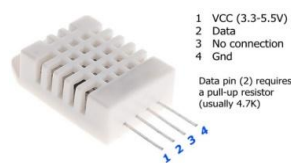


Fig. 3. DHT22 sensor and pin structure

C. Pressure Measurement

The BMP180 digital air pressure sensor image used for pressure measurement in the mobile meteorological station is given in Fig. 4.



Fig. 4. BMP180 digital air pressure sensor

The BMP180 digital pressure sensor is a useful product that digitally outputs the air pressure in the environment and also compatible with many microcontroller cards. It can measure the pressure value between 300 and 1100hPa, and give the height information between 500 and 9000 meters. Input voltage is 3.3V. It also supports the I2C protocol.

D. The speed of Wind Measurement

The wind sensor (anemometer) with analog voltage output is as shown in Fig. 5. It is used to measure the wind speed in the weather measurement stations. It is designed to work outdoors and has a water and rain resistant connector. To use this device, you can connect the black cable to the ground and brown cable to the 7-24V DC voltage to obtain the analog output from the blue cable. The output voltage is in the range of 0.4V to 2.0V and the winding measurement range is in the range of 0m/s to 50m/s. In addition, wind measurement sensitivity is 0.1m/s.



Fig. 5. The sensor used for wind measurement (Anemometer)

E. Memory (SD Card) Module

The SD card module used in Fig. 6 was used to record the measurement results from the temperature, humidity, pressure and wind sensors.



Fig. 6. SD card module used to record measurement results

III. DESIGNED MOBILE METEOROLOGICAL STATION SYSTEM

Arduino Mega 2560 embedded system control card is used as a central control unit in the mobile design. DHT22 temperature and humidity sensor, BMP180 digital air pressure sensor and Analog Voltage Output Wind Sensor (Anemometer) are used to measure air changes such as temperature, humidity, pressure and wind speeds. The mobile meteorological station designed was established on the Faculty of Engineering and measurements were taken. Photographs of the mobile meteorological station established for measurement are shown in Fig. 7.



Fig. 7. Photos of the designed system at the measuring point

Measurement controls are controlled via the workstation and calibration settings are made. Sensitivity and time settings have been performed on the workstation before the exact measurements have been made. The energy requirement of the station was met by a battery. While the measurements were continued, controls were made occasionally over the workstation and the energy conditions of the batteries were checked. These measured parameters were recorded in an SD card memory unit and transferred to the workstation at from time to time.

IV. RESULTS OF MEASUREMENT

Within the scope of this study, an embedded system controlled mobile meteorological station was designed and implemented. Temperature, humidity, pressure and wind measurements were performed in the Karamanoğlu Mehmetbey University Yunus Emre Campus. The wind, humidity, pressure, and temperature values were measured and the data set was formed from the measurements. Measurements were made and recorded for each minute, also daily averages were taken within this period. Some values of these measurements are given in Table-2.

TABLE II. DATA SET OBTAINED AS A RESULT OF MEASUREMENTS

Year	Month	Day	Temperature [°C]	Pressure[hPa]	Humidity [%]	Wind [km/hour]
2018	6	1	19.7	900.6	59.3	0.6
2018	6	2	15.4	901.4	68.6	0.1
2018	6	3	17.3	900.1	71.5	0.5
2018	6	4	18.1	898.7	65.8	0.8
2018	6	5	18.3	898.2	62.1	0.6
2018	6	6	19.9	899.8	60.4	0.6
2018	6	7	20.7	902.1	61.7	0.6
2018	6	8	22.8	899.2	54.8	0.7
2018	6	9	23.5	897.2	43	1.0
2018	6	10	21	896.2	44.9	0.9
2018	7	11	27.3	896.5	38.4	1.4
2018	7	12	25.3	895.5	50.6	1.4
2018	7	13	24.5	897.4	43.8	1.6
2018	7	14	26	897.4	37.6	0.6
2018	7	15	26.3	898.6	38.6	1.2
2018	7	16	26.4	899.3	39	1.3
2018	7	17	24.8	900.2	37.4	1.9
2018	7	18	24.3	899.2	42.5	1.3
2018	7	19	25.7	898.5	35	1.2
2018	7	20	26.6	896	32.6	0.6
2018	8	21	30.9	897.1	33.4	0.5
2018	8	22	30.1	895.2	37.3	0.7
2018	8	23	27.7	894.7	45.3	0.8
2018	8	24	24.6	896.9	51.8	0.9
2018	8	25	23.5	898.8	38.1	1.5
2018	8	26	22.2	899.5	36.9	1.5
2018	8	27	22.8	900.8	41.9	1.2
2018	8	28	23.3	902.4	43.5	0.8
2018	8	29	22.4	902.5	37.6	1.7
2018	8	30	23.3	901.4	38.2	1.9

V. CONCLUSION

Within the scope of this study, an embedded system controlled mobile meteorological station was designed and implemented. Temperature, humidity, pressure and wind measurements were performed in the Karamanoğlu Mehmetbey University Yunus Emre Campus. Wind, Humidity, Pressure, and Temperature values were measured and the data set was formed from the measurements. Measurements were made and recorded for each minute, also daily averages were taken within this period. In the next phase of this project, longer-term measurements will be made to expand the data set. Measurements can be made by means of Temperature, Humidity, Wind or Pressure values. Besides this, estimates can be made from the data set in regions where adequate measurements cannot be obtained for forecasting the weather.

ACKNOWLEDGMENT

This study was supported by Karamanoğlu Mehmetbey University Scientific Research Projects Unit 03-M-17.

REFERENCES

- [1] H. R. Byers, "General meteorology," McGraw-Hill New York, vol. 46, 1959.
- [2] C. R. Stearns, L. M. Keller, G. A. Weidner, M. Sievers, "Monthly mean climatic data for Antarctic automatic weather stations," Antarctic meteorology and climatology: studies based on automatic weather stations, vol. 61, 1993, pp.1-21.
- [3] C. Rosenzweig, et al. "Climate change and extreme weather events; implications for food production, plant diseases, and pests," Global change & human health 2.2, 2001, pp.90-104.
- [4] K. E. Kunkel, P. A. Roger, and A. C. Stanley, "Temporal fluctuations in weather and climate extremes that cause economic and human health impacts: A review," Bulletin of the American Meteorological Society 80.6, 1999, pp.1077-1098.
- [5] H. S. Bagiorgas, et al. "The design, installation and operation of a fully computerized, Automatic Weather Station for high quality Meteorological measurements," Fresenius Environmental Bulletin 16.8, 2007 pp.948-962.
- [6] TheEngineeringProject– Tutorial & Project for engineers web site from <https://www.theengineeringprojects.com/2018/06/introduction-to-arduino-mega-2560.html>